minerals

MDPI

Review

Mineralogical Investigation of Riverine Suspended Particulate Matter: A Comprehensive Review of Sampling, Characterization and Analytical Techniques

Mathieu Le Meur [1,*], Phu Le Vo [2,3], Au Hai Nguyen [3,4] and Hussein J. Kanbar [5]

[1] EPOC (UMR 5805), CNRS, Bordeaux INP, ENSEGID, 1 Allée, Fernand Daguin, 33600 Pessac, France
[2] Faculty of Environment and Natural Resources, Ho Chi Minh City University of Technology (HCMUT), 268 Ly Thuong Kiet Street, Dien Hong Ward, Ho Chi Minh City 70000, Vietnam; volephu@hcmut.edu.vn
[3] Institute of Environment and Natural Resources (IER), Vietnam National University Ho Chi Minh (VNU-HCM), Vo Truong Toan Street, Linh Xuan Ward, Ho Chi Minh City 70000, Vietnam; haiauvtn@gmail.com
[4] Department Informatics, Natural Resources and Environment (DINRE), Institute for Environment and Resources (IER), 142 To Hien Thanh Street, District 10, Ho Chi Minh City 70000, Vietnam
[5] The Interdisciplinary Center for Archaeology and the Evolution of Human Behaviour (ICArEHB), Universidade do Algarve, Campus de Gambelas, 8005-139 Faro, Portugal; hsen.kanbar@gmail.com
* Correspondence: mathieu.le_meur@bordeaux-inp.fr

Abstract

Suspended particulate matter (SPM) governs the transport of sediments, nutrients, trace elements, radionuclides, and organic contaminants in water bodies, largely through its mineral fraction, which controls contaminant mobility and bioavailability. Characterizing this fraction remains challenging because of small particle size, complex organo-mineral associations, poor crystallinity, and the dynamic nature of aquatic particles. This review critically compares the principal sampling strategies and analytical techniques available for investigating the mineral fraction of riverine SPM, from bulk approaches (specific surface area, elemental and mineralogical analyses) to particle- and atomic-scale methods (manual and automated electron microscopy, X-ray absorption spectroscopy, isotopic analyses). For each technique, we synthesize the information it provides, its sample-preparation constraints and artefacts, and its complementarity with other methods, summarized in a comparative table. We show that no single technique is sufficient to characterize natural SPM. Only the integration of complementary methods across spatial scales provides a robust framework for understanding particle composition, reactivity, and contaminant dynamics. We further highlight emerging opportunities offered by in-situ and autonomous sampling technologies, cryogenic and in-situ electron microscopy, and machine-learning-based multimodal data fusion. Future progress will depend on harmonized sampling and analytical protocols, international SPM databases, and combined laboratory-field approaches.

Keywords: SPM; sampling techniques; bulk mineral characterization; atomic-scale characterization; particulate mineral characterization

Academic Editor: Niloofar Karimian

Received: 3 August 2026
Revised: 4 September 2026
Accepted: 15 September 2026
Published: 17 September 2026

1. Introduction

River suspended particulate matter (SPM) is composed of colloids (1 nm–1 µm) and particles (>1 µm), forming complex and heterogeneous aggregates of mineral, organic, and microbiological components [1]. In addition, SPM is defined as any material in aquatic systems that does not settle and is retained by filtration over a 0.45 or 0.22 µm pore-size

membrane [2]. In natural aquatic systems, these components are frequently formed into floc-like structures whose composition, density, size, and reactivity continuously evolve according to hydrological, physicochemical, and biological conditions [3–5]. Consequently, the study of SPM is inherently interdisciplinary and requires combined physical, chemical, and mineralogical approaches to decipher their whole complexity.

Compared with soils and sediments, studies focusing on freshwater SPM [6] remain relatively limited due to their high mobility, reactivity, and difficulty to sample. Their transient nature, rapid aggregation/disaggregation processes, and strong spatial and temporal variability considerably complicate both field investigations and laboratory analyses [7,8]. However, increasing efforts have recently been devoted to the development and adaptation of techniques suitable for sampling and characterizing natural SPM in aquatic systems.

Rivers and streams constitute the principal vectors of matter fluxes within watersheds and may therefore be considered as the ecological arteries of catchments. SPM enters river systems through multiple mechanisms including soil erosion, runoff, bank erosion, atmospheric deposition, wastewater discharge, mining activities, and sediment resuspension (Figure 1). The transport of SPM plays a major role in regional and global biogeochemical cycles by facilitating the transfer of carbon, nutrients, trace elements, and contaminants between terrestrial and aquatic environments [9,10]. This is mainly because SPM, due to its fine texture, can hold and transport nutrients and contaminants for long distances in water systems [11]. Investigating SPM transport in river catchments is a key component of the environmental monitoring of large and small rivers, as they may cause important environmental impacts [12,13]. Suspended particulate matter transport can have impacts on: (i) water turbidity, (ii) fish habitats [14], (iii) siltation of reservoirs [15], (iv) transport of contaminants such as polychlorinated biphenyls (PCBs), trace metal elements (TME), radionuclides, or nutrients [16–18].

Transport of SPM from land to ocean is estimated between 12.6 and 24 Gt year^{-1} [12], with a frequently observed value of 15 Gt year^{-1} in the literature [19]. However, this value is associated with uncertainties and does not take into account recent anthropogenic activities (deforestation, agriculture, mining, urbanization) and/or climate change [20]. The nature and amount of particles in rivers are controlled by the weathering regime. Fast mechanical weathering will engender immature particles and quartz, K-feldspar, illite, calcite, and kaolinite [21]. By contrast, fast chemical weathering will permit the formation of mature particles: poorly ordered kaolinite, goethite, and particulate organic matter [22]. The weathering regime is governed by the climate through different processes such as relief, surface area of the catchment, geology, vegetation, as well as human activities [19,23].

Because of their high specific surface area (SSA) and strong adsorption capacity, SPM also acts as an important carrier for contaminants in aquatic environments [24,25]. Toxic metals, radionuclides, organic contaminants, and pathogenic microorganisms originating from both natural and anthropogenic sources may adsorb onto particle surfaces, undergo physicochemical transformations, and subsequently be transported, remobilized, or released within aquatic systems [26]. The interactions between mineral particles, natural organic matter, and biological components strongly influence aggregation mechanisms, contaminant binding, and particle stability.

The mineral fraction of SPM is of particular importance because mineral surfaces largely govern adsorption mechanisms, redox reactions, aggregation behavior, and contaminant mobility. Clay minerals are omnipresent in SPM (22–72%wt). Feldspars and carbonates are also reported (61%wt) but can be absent due to dissolution in the watercourse [27]. Quartz and feldspars, respectively, can represent 8–35%wt and 4–41%wt in SPM. This proportion can highly vary based on water discharge [28,29]. Oxides and (oxy)hydroxides (mainly FeOx) are also reported in the literature but in lower amounts.

FeOx are present as "patchy coatings" on other minerals [30,31]. Co-occurrence of Fe with Al, Si, Ca, and discrete FeOx particles is also reported [32–34]. Amorphous phases, ferrihydrite, goethite, and hematite are frequently reported in the literature [33,35–38]. Clay minerals, iron and manganese oxides, carbonates, silicates, and authigenic mineral phases may coexist within highly heterogeneous particle assemblages and strongly influence the environmental reactivity of suspended particles [6]. However, the characterization of these mineral phases remains challenging because of their small size, low abundance, poor crystallinity, and intimate association with organic and biological materials.

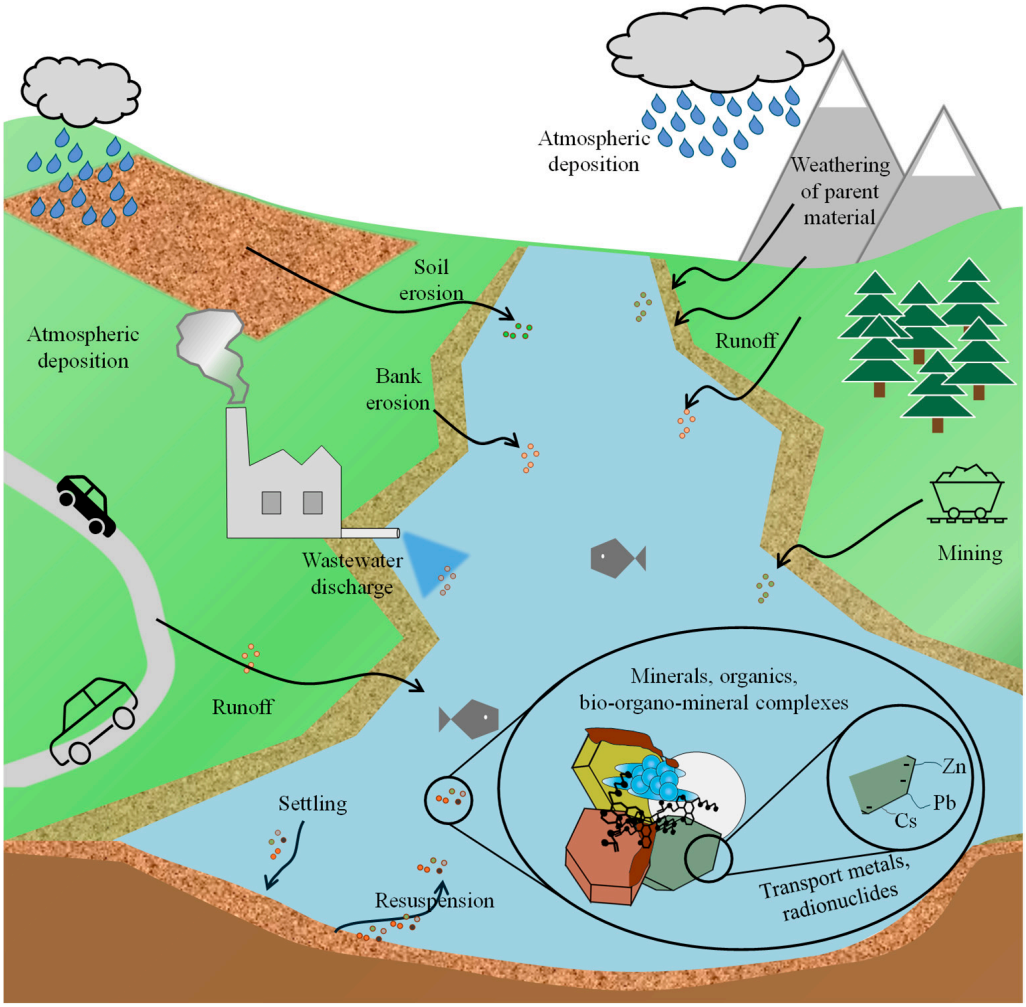

Figure 1. Sources and fate of SPM in the watershed. Circles represent SPM derived from different sources and pathways, comprising heterogeneous mixtures of mineral, organic, and biological components (bio-organo-mineral complexes), as illustrated in the magnified view. These complexes can retain and transport metals, radionuclides, and other contaminants, thereby influencing their fate and mobility within the watershed.

Riverine suspended particulate matter (SPM) plays a crucial role in biogeochemical cycling and contaminant dynamics within aquatic systems, particularly in inland waters and estuaries where particle concentrations are significantly higher than in the open ocean [39]. Recent advances in high-resolution analytical techniques, including synchrotron-based approaches, electron microscopy, and coupled spectroscopic-imaging methods, have dramatically improved our ability to characterize mineral speciation, particle heterogeneity, and organo-mineral associations at multiple scales. These tools have revealed substantial disparities between natural SPM and simplified laboratory analogues regarding metal

reactivity [37], underscoring the urgent need to investigate natural particulate systems under environmentally relevant conditions.

While several reviews have addressed specific aspects of SPM research, such as flocculation dynamics [6,7], contaminant transport [17,18,40], or individual analytical techniques [41–43], very few comprehensive syntheses systematically evaluate the full methodological workflow from sampling to high-resolution mineral characterization [44]. Existing reviews tend to focus on either bulk geochemical approaches [27,45] or specialized techniques [46,47], offering little practical guidance on method integration or interpretation for researchers new to the field or seeking to expand their toolkit.

This review fills that gap by providing a critical, comparative assessment of the complete analytical pipeline for investigating the mineral fraction of riverine SPM. Specifically, we (i) evaluate sampling strategies and their associated artifacts, (ii) systematically compare bulk versus particle-scale analytical techniques, (iii) identify common pitfalls in sample preparation and data interpretation, and (iv) offer actionable recommendations for method selection and integration. We pay special attention to how methodological choices influence the interpretation of mineralogical composition, particle reactivity, and contaminant binding.

This review aims to improve the quality, consistency, and global comparability of SPM mineralogy studies and is designed for researchers at all career stages, from novices seeking a methodological roadmap to experienced investigators looking to expand their toolkit or grasp the limits of unfamiliar techniques. The paper is structured as follows: the first section covers principal SPM sampling methods; the second provides a detailed (though non-exhaustive) overview of current analytical techniques, ranging from bulk approaches to high-resolution analyses; and we conclude with a Critical Synthesis and Comparison of Analytical Approaches and discuss future perspectives and outstanding challenges in SPM research.

2. Sampling Techniques to Collect SPM

It is crucial to obtain a representative SPM sample to describe the chemical and physical state of a catchment. SPM sampling is an essential step to ensure the success of its characterization. In particular, contamination can occur due to careless handling or improper protocol preparation. In the literature, different techniques are described for SPM sampling, such as direct water sampling followed by filtration [48], in-line filtration [49], continuous flow centrifugation [50], particle traps [51], and in-situ and autonomous sampling technologies [52,53]. They differ in terms of duration, yield, and sample composition [54].

2.1. Filtration Technique

The filtration technique is a widely used technique that separates the SPM from the water (except the colloids) [55]. Usually, 0.45 µm pore size filters are used (Figure 2). However, this technique is not truly representative because the sample volume is generally small (few liters) and the sampling time is very short. In addition, the SPM composition on the filter is altered; the SPM is aggregated and clogged on the filter compared to the SPM in the water column [56]. Finally, huge volumes of water need to be filtered to collect enough material (>2 g dry weight, d.w.) for exhaustive analyses of SPM [57]. For that purpose, this technique is only used when the other techniques described below are not feasible [54].

Technique	Separation based on	Pros	Cons	Application
 Filtration	Size of filter	Portable and easy setup Full recovery of particles (above filter pore size) Requires minimal tools Suitable for field screening and quick survey	Colloids lost during filtration Small sample volume (not representative) Small recovered SPM mass Chemical interactions may alter SPM Filter clogging reduces efficiency	Quick Survey and screening
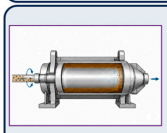 Continuous flow centrifuge	SPM size and density	High SPM material collection High retention yield (~90–98%) Can capture nanoparticles (~160nm) at >90% Mobile setup Can process large water volumes	Needs to be installed on site (voluminous) Grain size not representative (cut off ~1µm) Time consuming and expensive Requires power supply Maintenance-intensive Possible contamination from CFC	When high mass of material is needed
 Hydrocyclone	SPM size and density	High SPM material collection High retention yield (~70%) Continuous operation possible No moving parts (low mechanical failure)	Needs to be installed on site (voluminous) Isolates mainly heavy particles Time consuming and expensive Calibration needed for particle size Limited efficiency for fine particles	When continuous operation is needed
 Sedimentation trap	River velocity	Low cost Easy to set up Long-term deployment feasible	Representativeness questionable Grain size not representative Flow turbulence alters settling rate	Long term monitoring
 Field flow fractionation	Size and density	High precision and preservation of particles Effective for colloid collection Minimal damage to particles Allows coupling with detectors (e.g., UV, fluorescence)	Requires trained personnel Small sample volume Expensive Particles range 1nm–100µm Large particles can clog channel Requires maintenance	Assess UV or fluorescence information
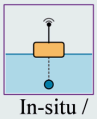 In-situ / autonomous sensors	Continuous monitoring (no sampling nor separation)	Continuous / high-frequency data No power-intensive collection Captures short-term variability Can trigger autonomous sampling Low-cost sensor networks Feasible	No physical sample obtained Needs calibration against gravimetric/mineralogical references Optical/acoustic proxies only Coarse particle-size information only	Continuous monitoring and sampling triggers

Figure 2. The various techniques that are used for SPM collection.

2.2. The Continuous Flow Centrifugation (CFC)

Continuous flow centrifugation is a well-established and reliable technique to collect SPM [58,59]. This technique separates the SPM from the water phase at a defined constant throughput. CFC separates particles according to size and density, such as natural sedimentation process [55]. The water is pumped from the river, and the SPM is deposited on the inner wall of the rotating cylinder. In order to facilitate the SPM recovery, Teflon plates are installed in the bowl to attach the SPM [37]. The separation efficiency can reach 90%–98% [60]. One of the advantages of this technique is that the sample yield is considerably higher than filtration (several grams) and therefore permits a better comprehension of chemical, physical, and mineralogical characterization of the suspended material collected. The CFC can be installed at a monitoring station, on a trailer, or on a boat and can be mobile; however, this technique is voluminous and requires large and stable riverbanks. This technique is grain size dependent, and the density between water and SPM also influences the sampling [61]. In addition, different grain size classes may be lost [62] (the average cut-off is 1 µm). This information can, in certain cases, be crucial, for example, in the analyses of Polycyclic Aromatic Hydrocarbons (PAH) on SPM [63]. However, ref. [64] showed that CFC can retain nanoparticles (~160 nm) with high efficiency (>90%). This technique is also time-consuming and expensive. Thus, it is difficult to investigate the spatial and temporal variability of SPM [65]. Finally, there is a possibility of contamination

from CFC components (e.g., bearings, lubrication oil) [66,67] and physical effects during centrifugation, such as changes in cut-off due to the bowl filling up or fragmentation and aggregation of particles (shear stress).

2.3. Hydrocyclone (HC)

The hydrocyclone is a device widely used in petroleum, mineral, and environmental engineering. Surprisingly, this technique is not widely reported in the literature [68]. SPM is separated from water in the HC using centrifugal force. A high flow rate of water is introduced into the upper cylinder. This water is then forced into a downward vortex. Due to the centrifugal forces, the particles are pressed against the wall where they are collected [61]. Several studies showed that HC systems can retain ~75% of SPM in the size range 20–30 µm at a very high throughput [61,69]. Ref. [64] compared CFC and HC and concluded that both of these techniques worked well under real work conditions.

2.4. The Sedimentation Trap (ST)

The sedimentation trap is a technique that uses the natural velocity of the river to collect particles via sedimentation in the interior of the trap. This technique is also called "fresh sediment derived from suspended solids" [70]. It is a low-cost technique that can be easily set up and does not require attendance. This method also integrates a longer period of time (1 to 4 weeks typically) that is well-suited for in situ monitoring over a year [65,71]. Whereas the sampling of SPM by CFC has been investigated and validated since the 1990s (see above), the representativeness of the SPM collected with STs is still questionable. Several studies showed that SPM sampled by STs differs from river SPM in grain size distribution and organic carbon content [51]. The fine particulate matter can be lost with the overflow [54,70], and the SPM concentration in the water column is not available. This difference could lead to biased concentrations for contaminants [72]. In their study, ref. [57] showed a difference in grain-size distribution between SPM collected by sediment traps (0.1–400 µm) and CFC (0.1–112 µm). They also observed seasonal differences in particulate organic carbon concentrations due to degradation or phytoplankton blooms. However, they concluded that ST sampling is a valuable technique to assess spatial and temporal trends of particulate contaminants (PCBs and Hg).

2.5. Colloid Separation and Other Techniques

The use of filtration or centrifugation in the field cannot entirely certify the separation of colloids and particles. Field-flow fractionation (FFF) is a relatively new technique that is capable of high-resolution separation of colloids and inorganic particles [73]. The two main principles are sedimentation (SedFFF) and asymmetric flow field-flow fractionation. The separation is achieved by the interaction of sample components with an externally generated field that is applied perpendicularly to the direction of the mobile phase flow. It can also be coupled with a second cross-flow stream, resulting in flow field-flow fractionation with better separation [74,75]. This rapid technique (10–30 min) permits the separation of a continuous large class of particles (from ~1 nm to 100 µm) and is based on important properties such as their surface charge, density, size, shape, and diffusion coefficient [73,76]. This method has been employed, coupled with different detectors (fluorescence, UV absorbance) for river colloids [77]. A good introduction to the FFF theory can be found in the literature [78].

Different studies in the literature try to compare different devices based on the difference between passive sampling and active sampling. Passive sampling methods are based on lowering the flow speed of the water inside the sample. On the other hand, active sampling is based on applying external force to separate SPM from water [79]. For example, ref. [61] compared the efficiency of time-integrated sampling devices (Binnensammler

device and Phillips sampler, PS) and discrete sampling devices (CFC and Hydrocyclone, HC). They showed similar physical and chemical parameters for the two time-integrating sampling devices, as well as organic pollutants. However, they remarked differences in TOC concentrations between CFC and PS due to degradation processes occurring in the PS device. Figure 2 shows the advantages and limitations of the different sampling techniques. Recently, systematic validation of these approaches has highlighted critical technical biases. Another study [79] demonstrated that passive devices (such as sedimentation boxes or tanks) significantly underestimate fine particles (<75 μm) and low-density microplastics (<80 μm, with a capture efficiency below 20%), shifting the collected grain-size distribution toward coarser fractions compared to active CFC or filtration methods. Despite these physical limitations, sedimentation boxes remain highly valuable for integrating fluxes over several weeks. Each technique has its benefits and limitations (size range collected; retention capacity of particles). It is then of pivotal importance to carefully consider SPM sampling efficiencies of the device used, especially when dealing with a quantitative approach.

2.6. Complementary In-Situ Monitoring and Autonomous Sampling Technologies for SPM

Beyond discrete sampling campaigns, a growing set of in-situ and autonomous technologies now allows continuous or high-frequency monitoring (but not collection) of SPM, addressing the strong short-term variability that discrete sampling cannot resolve [52,53]. Optical and acoustic turbidity probes, laser in-situ scattering and transmissometry (LISST) instruments, and low-cost open-source turbidity sensors can be deployed at fixed stations or on mobile platforms to record SPM concentration and, for LISST-type instruments, particle-size distribution at sub-hourly resolution over months [80,81]. Networks of low-cost sensors are increasingly used to characterize the spatial heterogeneity of sediment sources and transport within river networks, complementing the limited number of sites that can be instrumented with expensive reference-grade probes. For instance, ref. [81] developed and validated an open-source turbidity sensor that achieves precise, reproducible measurements across a wide concentration range, demonstrating its viability for distributed monitoring applications. However, optical proxies require careful site-specific calibration: [82], for example, demonstrated that the turbidity-suspended sediment concentration correlation depends on sediment composition and particle size distribution. Autonomous samplers that combine flow, turbidity, and depth measurements to trigger sample collection at target concentrations or discharge thresholds can further improve the representativeness of the samples subsequently used for mineralogical analysis [80]. A more comprehensive example is the RIPLE platform developed by [83], which integrates turbidimeters, automatic samplers, and bedload sensors into a single solar-powered device for high-frequency monitoring of water and sediment fluxes in mesoscale rivers. This demonstrates the growing capability of autonomous systems to capture the full spectrum of sediment transport dynamics. However, these technologies generally provide only bulk concentration or optically-derived proxies of SPM rather than a physical sample suitable for direct mineralogical characterization, and their outputs require calibration against gravimetric and mineralogical reference measurements. Therefore, they are regarded as complementary to the SPM sampling techniques described above.

3. Characterization of SPM (Mineral Fraction) at Bulk, Particulate, and Atomic Scales

Global characterization of the physical and chemical fraction of SPM is not possible via one technique. Different techniques are complementary and permit a better understand-

ing of the whole complexity of natural SPM and their reactivity towards contaminants (Figure 3).

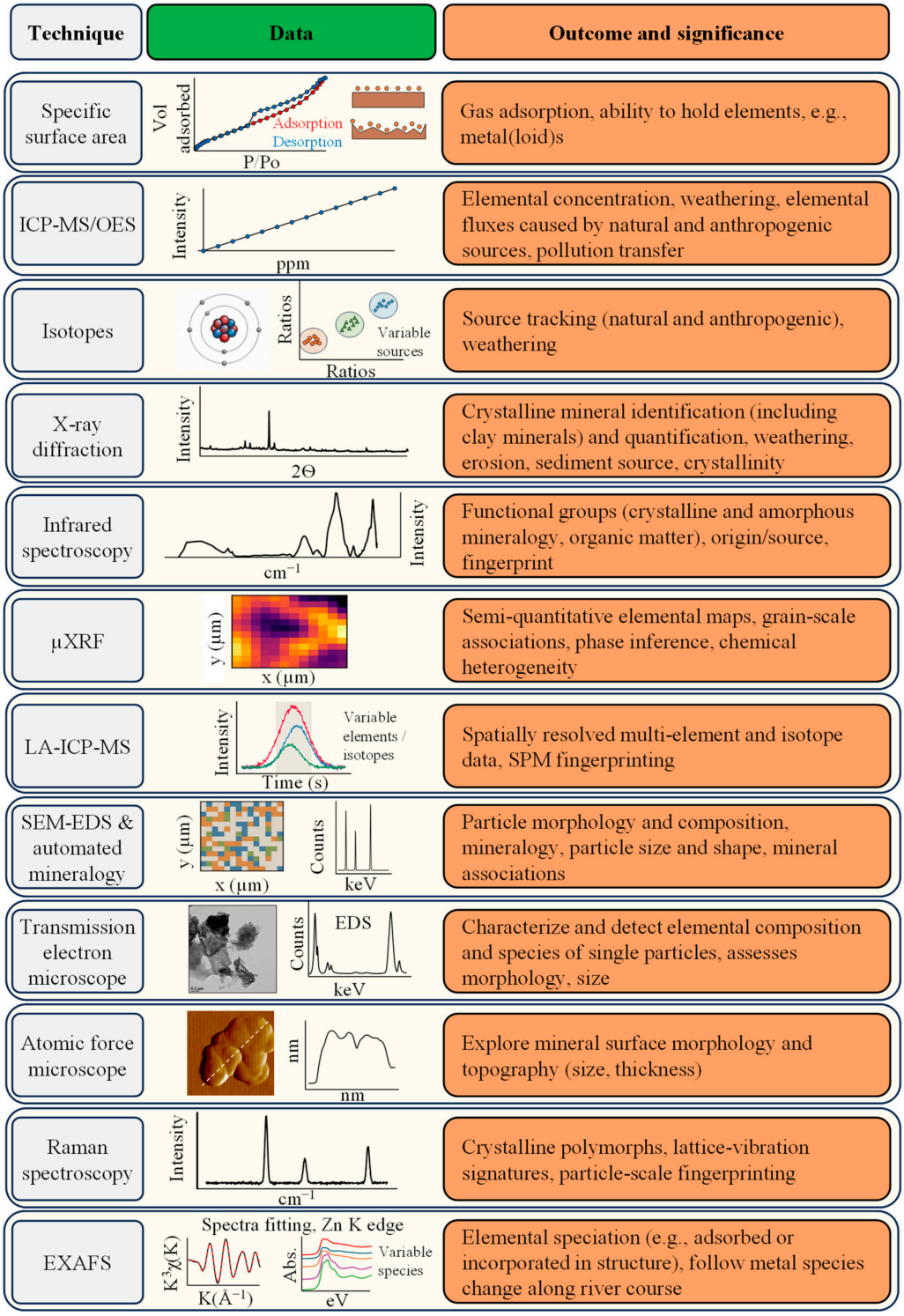

Figure 3. Main analytical techniques and tools that are used for SPM characterization. Within the "Data" column, colors represent different samples or sources (e.g., isotopes), and schematic lines and shapes illustrate the corresponding analytical signals.

3.1. Specific Surface Area

The Specific surface area (SSA) is a pivotal parameter to better understand the processes that occur at the mineral interface [84]. A routine method for SSA determination

of fine grains, such as SPM, is the gas adsorption method. The analysis of the adsorption isotherm of a non-polar gas such as N_2, Ar, Kr, or CO_2 permits the calculation of the surface area of SPM (i.e., the surface ideally covered by a monolayer of adsorbed gas). The measurement of SSA is determined by the BET (Brunauer-Emmett-Teller) method [85]. Microporous surface (pore size ranging from 0.8–2 nm) is obtained by the t-plot method [86], and mesoporous distribution size (pore size ranging from 2 to 80 nm) is determined by the BJH method [87]. The meso- and micropores are evaluated by the hysteresis of the adsorption and desorption isotherm. Prior to measurement, this method requires the total removal of adsorbed surface water and interlayer cations [88,89]. However, in the case of natural particles, the temperature of outgassing is crucial, as it could alter iron (hydro)oxide [90]. For bulk samples, such as SPM, the adsorption of liquid ethylene glycol monomethyl ether (EGME) can be an alternative. Indeed, EGME covers the external surface of particles and penetrates the interlayer space of swelling clay minerals [91].

The mineral fraction of SPM is mainly composed of clay minerals, which develop two kinds of surfaces: the basal (001) surface that carries negative charges and the edge or lateral surfaces that are pH-dependent [92]. Concerning clay minerals, the mesopores (2–50 nm) are mainly interparticle pores and have a minor effect on the gas adsorption surface area [93]. On the other hand, micropores (2 nm) result from the intraparticle space and are N_2-accessible [94]. For example, micropores in bentonites contribute significantly to the total SSA of gas adsorption measurements [93]. Ref. [95] characterized SPM from a New Zealand watershed and showed that SSA increased with increasing SPM concentration in relation to the increase in flow rate. The result commonly observed for environmental particles is a surface area increase with fine particles, such as clays that have a high surface area-to-volume ratio [96]. This larger surface area facilitates the sequestration of contaminants such as trace metals [95,97]. More recently, ref. [6] highlighted that the SSA of natural SPM is highly dynamic and closely linked to flocculation processes. They demonstrated that the adsorption of natural organic matter (NOM) can either clog mineral pores, reducing the measurable BET surface area, or create new complex organo-mineral micro-architectures that modify the overall particle porosity and reactivity. The interaction between FeOx and phyllosilicates is more studied in the case of natural SPM. This interaction favors flocculation and enhances the surface area of SPM, as suggested by several authors [30,33,98]. Ref. [30] showed a close relationship between iron oxide content and surface area when interacting with clay minerals. They argue that this relationship could be the result of the abundance of edge sites for electrostatic attraction between iron and clay [97]. Ref. [31] also studied the SSA of natural particles from the Moselle River (France). They showed that the SSA of natural particles ranged between 6 and 37 $m^2\ g^{-1}$, and organic matter content increased the mean particle size and decreased the SSA. In addition, no significant microporous surface area was measured ($\leq$1 $m^2\ g^{-1}$).

3.2. Bulk Chemical Analyses

3.2.1. Elemental Analysis by ICP-MS and ICP-OES

Bulk chemical or elemental analyses are often conducted to quantify the full spectrum of non-metallic, metalloid, and metallic elements in natural SPM [99]. In environmental laboratories, ICP-MS and ICP-OES are the two most advanced elemental analysis techniques routinely used [100]; the selection of the method depends on the elemental content range (i.e., ICP-MS for ppt range and ICP-OES for ppb as well as ppm [45]. Before any preparation, it is necessary to use trace metal grade acids and solvents, as well as vessels that have been soaked and rinsed with deionized water. This is because deionized water is free of impurities, including metal ions [101]. SPM, as solid samples, must encompass different steps, including drying, grinding, sieving, acid digestion, filtration, and occa-

sionally pre-concentration techniques for homogenization before introduction into the ICP-OES [102,103]. Recent applications of ICP-OES and MS can be highly beneficial for the scientific community.

A critical, and often underreported, step for ICP-based analyses of SPM is the strategy used to bring the solid sample into solution, because this choice strongly conditions which elemental pools are actually measured. Two broad approaches are used: acid digestion, in which the sample is attacked with mixtures of strong acids (e.g., HF-HNO_3-$HClO_4$ or aqua regia), most often in closed microwave vessels for silicate-rich SPM. The second is alkaline fusion, in which the sample is fused with a flux (e.g., $LiBO_2$, Na_2O_2) at high temperature before dissolution [104]. However, these approaches are destructive, and therefore the samples cannot be recovered afterwards. Fusion generally achieves complete dissolution of resistant silicate and refractory oxide phases and is therefore required to obtain total elemental concentrations, but the high dilution factor and salt matrix it introduces can compromise trace-element detection limits and cause spectral and matrix interferences in ICP-MS. Acid digestion protocols that omit HF, or that rely on open-vessel, low-temperature digestion, typically achieve only partial (pseudo-total) extraction [105]. If the digestion is incomplete, the solution can form co-precipitates [106]. Acid digestion methods preferentially attack carbonates, (oxy)hydroxides, and organic matter while leaving detrital quartz, feldspars, and part of the phyllosilicate lattice undissolved, which can bias apparent elemental ratios and underestimate lithogenic elements such as Al and Si as well as structurally-bound trace metals. Because SPM commonly contains a substantial and variable organic matter content, an oxidative pre-treatment (e.g., H_2O_2) is often required before or during digestion to prevent interference with the subsequent acid attack and with plasma stability. Likewise, carbonate phases, when present, may need to be removed or quantified separately (e.g., by sequential or selective extraction) if the objective is to isolate the silicate-bound elemental fraction. Contamination control is equally critical given the small sample masses and low elemental concentrations typical of SPM: procedural blanks, certified reference materials processed alongside the samples, and duplicate digestions are the minimum QA/QC requirements needed to validate digestion recovery and analytical accuracy. Because digestion versus fusion and partial versus total extraction are not interchangeable, results should always be reported together with the digestion protocol used, since this choice can otherwise render elemental concentrations from different studies not directly comparable. The next paragraph presents non-exhaustive results concerning the applications for riverine SPM studies.

Many studies dealing with elemental analysis of natural SPM can be encountered in the literature worldwide. For example, ref. [37] investigated the spatial and temporal variability of SPM in the Moselle River (France). They showed an urbanization gradient in the downstream direction of the Moselle River and a seasonal variation with more silty particles during high-flow regimes. Ref. [107] studied the suspended load of the Ganga and Brahmaputra Rivers using a combination of techniques in order to achieve maximum precision in the identification of the different size fractions. The geochemistry using ICP-MS showed that the surface load was enriched in metals. They also showed that the chemical variability of suspended load is influenced by hydraulic, weathering, and possibly anthropic effects. Refs. [19,108] presented a database of the chemical composition of SPM in World Rivers and gave a snapshot of elemental fluxes for different continents. Ref. [19] found that the anthropogenic fluxes and riverine fluxes are similar, revealing that human activities have effects on the cycles of trace elements. Ref. [109] analyzed SPM from the Yarlung Tsanpo River (Tibetan Plateau); they selected 10 metal(loid)s (V, Cr, Co, Ni, Cu, Zn, As, Cd, Sb, Cs) and analyzed them by ICP-OES and ICP-MS. They measured the highest enrichment values for Cu, As, and Cd. They showed seasonal enrichment due to

hydrodynamic conditions. They also showed that SPM is mainly anthropogenic and from geothermal activities. Ref. [110] measured the impacts of the human-induced flood event on heavy metal transport, spatiotemporal variations in contents and fluxes of metals (Cr, Ni, Cu, Zn, As, Cd) using ICP-MS. They concluded that metal transport was controlled by hydrological processes and dominated by SPM, with strong association with particle size and SPM concentration.

3.2.2. Isotopic Fingerprinting

Isotopes are atoms of an element that differ in their number of neutrons and thus have different masses. They can be classified into radioisotopes and stable isotopes [47,111]. Stable isotopes are divided into traditional stable isotopes (C, H, O, N, S) and non-traditional stable isotopes (Pb, Cu, Zn, Cd, Hg, Cr, Mg) [112,113]. They are high atomic weight, have a small mass difference between isotopes, and are in the form of ionic bonds [47]. The international nomenclature is expressed as delta values, δ. It is a relative value compared to reference materials in order to compare the results between laboratories, where the common material is the zero baseline [47]. Positive and negative values of δ indicate the relative enrichment of heavy and light isotopes. In the periodic table, only 21 elements are composed of only one stable isotope (e.g., Na, Al, P, Mn), permitting the use of a large panel of elements.

Mass spectrometry is the technique of choice for high-accuracy isotope composition detection. The ionization mechanism permits classification of different MS techniques: (i) isotope ratio mass spectrometry (IRMS), (ii) thermoelectric ionization mass spectrometry (TIMS), and (iii) inductively coupled plasma mass spectrometry (MC-ICP-MS) [114–117]. IRMS is used for light gaseous elements, while TIMS is used for heavy elements [47]. The analysis of many elements cannot be performed by IRMS and TIMS due to their low ionization efficiency. The use of MC-ICP-MS can analyze most elements with higher accuracy. The laser ablation multi-collector inductively coupled plasma mass spectrometer (LA-MC-ICP-MS) is gradually being adopted [118]. Laser ablation permits sputtering atoms from the surface and then transporting them to the plasma for ionization. However, the instrument mass bias from laser-induced isotope fractionation is difficult to manage for accurate isotope determination.

This difference in mass causes slight differences in reactivity, giving this technique a strong advantage for better understanding the SPM behavior in the water column. The different signatures of the element isotopes can give information on source tracing. This application is based on the mixing of reservoirs with different isotope signatures. If the isotopic compositions of the involved endmembers are known and the contributions of different source materials are distinct, mixing calculations can help unravel the different sources of SPM. Metal isotopes can be measured using an MC-ICP-MS instrument [111].

The sampling operation is crucial as it is necessary to minimize the interference from metal impurities. Therefore, laboratory procedures are strict. The preparation is performed in a cleanroom equipped with a Class 100 laminar flow exhaust hood and a positive-pressure room to prevent the entry of unpurified air from the exterior [119]. Chemicals used should be double distilled, and the instruments used should undergo acid washing and rinsing with ultrapure water [120]. The preparation procedure is not the same for liquids and solids. Concerning SPM, samples are ground and sifted before digestion. HF is mainly used to dissolve silicates in samples, and $HClO_4$ and H_2O_2 are used to remove organic matter from the sample [120,121]. Before analysis, the targeted element must be separated and purified from the matrix. The common separations are (i) precipitation, (ii) liquid extraction, (iii) chelating resin, and (iv) ion exchange chromatography [111,122].

Ion exchange chromatography is based on the ion exchange reactions between the sample and the resin.

Isotopic fractionation is the process that changes the relative abundance of stable isotopes of an element. This change is mostly very small, and the isotopic mass balance of the overall system remains unchanged. In addition, it is necessary to know that an enrichment in a certain reservoir must always be balanced by a corresponding depletion in another reservoir. Isotopic fractionation occurs during chemical, physical, and biological processes; two main mechanisms can cause isotopic fractionation, which are (i) the kinetic isotope effect and (ii) the thermodynamic isotope effect [111].

As this paper is dedicated to characterization techniques of SPM, we will present only two stable isotopes that are studied for source contamination investigation. Zinc (Zn) has five stable isotopes (^{64}Zn, ^{66}Zn, ^{67}Zn, ^{68}Zn, and ^{70}Zn) [123]. It is one of the major elements in aquatic systems. The low-temperature biogeochemical processes (absorption, desorption, dissolution, and precipitation) can induce Zn isotopic fractionation [124,125]. Relatively limited research focuses on δ^{66}Zn for SPM in rivers. The range of δ^{66}Zn varies from +0.2–0.35 ‰ [126]. These values are mainly reported from continental weathering. One of the earliest studies concerning Zn isotopes was in the Scheldt River estuary, with δ^{66}Zn values ranging from 0.21–1.13 ‰ [127]. Other examples show that δ^{66}Zn values range from 0.08–0.27 ‰ in the Seine River [125]. Additionally, the Zhujiang River Basin exhibited δ^{66}Zn values ranging from −0.11‰ to 0.41‰ [128]. It can be seen that ^{66}Zn enrichment is positively correlated with increasing downstream distance, resulting from Zn migration from the soil into the river system.

Copper (Cu) has two stable isotopes (^{63}Cu and ^{65}Cu), and Cu isotopic variation is described as $\delta^{65/63}$Cu [47]. Cu is a ubiquitous element, is naturally present in various environments, and plays a pivotal role in different environmental processes [129]. The factors inducing Cu isotopic fractionation at low temperature are (i) adsorption, (ii) conversion of Cu(I) and Cu(II), and (iii) mineral dissolution. Copper isotope fractionation was already reported for mine drainage [130] and to trace dissolved metal contaminants in streams affected by mining by-products [131]. Concerning the Yangtze River, we can observe an enrichment of heavier isotopes in the downstream direction of the river. The isotopic evaluation of Cu is rarely reported for SPM. Ref. [129] reported the Cu contents and Cu isotopic compositions of SPM in the Zhujiang River Basin. They measured a δ^{65}Cu value fluctuating between 0.04–0.50‰, with heavier isotopes downstream. Based on isotope ratios, they concluded that rock weathering contributed 76.4% of particulate Cu, and the contributions of urban sludge and smelting were 15.4% and 8.2%, respectively. A recent study [129] showed that δ^{65}Cu of SPM is mainly controlled by inorganic isotopic partitioning during weathering and transport. They also observed that the monsoon introduces lighter material, redefining the controls on Cu in large river systems.

3.3. Bulk Mineralogy and Vibrational Spectroscopy

3.3.1. X-Ray Diffraction (XRD)

After the characterization of bulk physical properties (SSA) and quantification of the elemental composition, the next conventional step in SPM characterization is mineral detection. Different techniques are available for mineral investigation in bulk natural SPM. XRD is a non-contact and non-destructive technique for a large panel of materials, including minerals [132]. XRD can identify and quantify crystalline mineral phases in SPM, such as primary and detrital minerals (quartz, phyllosilicates, and carbonates). It is easy to perform, quick, and can be used for other analyses, but requires at least tens to hundreds of milligrams. XRD complex diffractograms are modeled as a sum of individual mineral phases, and their relative abundances are refined by least-squares fitting of the entire

pattern, yielding the mass percentage of each component. Furthermore, the percentage of amorphous materials can also be quantified by using an internal standard [133]. Ref. [132] Additionally, XRD can measure the degree of orientation of clay particles and can thus, when coupled with electron microscopy, be used to investigate composite particles (individual particles of different mineralogy). XRD is also used to identify and distinguish between various clay minerals using oriented mounts. The main procedures rely on treating the material with ethylene glycol and heating the samples; this will lead to various swelling and collapse of the minerals [134,135]. X-ray diffraction has been used, for example, to follow the mineralogical evolution of river particles during a storm event with particles mainly composed of smectites [136]. Another study showed that during the beginning of the limb of the hydrograph, quartz is present as discrete particles, while at the end of the hydrograph, the SPM contains different particles of various sizes [137]. They concluded that XRD can be chosen as a tool to help guide the sampling procedure. Another study investigated the seasonal variations of SPM mineralogy of the lower Changjiang River using different techniques such as XRD [38]. They found a seasonal variation of clay mineralogy with distinct behaviors during the rainy season (more illite and less kaolinite proportion), suggesting more intense erosion in the basin during the rainy season. Ref. [138] studied the effect of flow rate and lithology on SPM mineralogy in Puerto Rican rivers using XRD. They showed that the mineralogy of suspended sediments in the three watersheds returned to baseline composition after storm events, showing the resilience of the watershed under strong hydrological conditions.

3.3.2. Fourier Transform Infrared Spectroscopy (FTIR)

Different spectroscopic methods are illustrated in the literature and can be used for particle characterization in bulk mode. This technique is also reported in order to fingerprint (i.e., source) sediments and SPM and is used as an alternative to traditional techniques such as geochemistry and the use of radionuclide tracers. Indeed, traditional tracers used for fingerprinting are time-consuming. Visible reflectance [139], visible near infrared (VNIR), shortwave infrared (SWIR) [140,141], diffuse reflectance infrared Fourier transform (DRIFT) spectroscopy [17,142], and near infrared (NIR) [143] are different techniques documented. FTIR technique can be performed in various modes, such as transmission mode, diffuse reflectance mode (DRIFT), and attenuated total reflectance (ATR).

Infrared spectroscopy (IR) is especially suitable to track mineral as well as organic compounds in SPM. A well-defined set of IR peaks can be used to identify organic matter and minerals, including clay minerals [144,145]. Additionally, IR can also be used to identify and distinguish between various carbonates, such as calcite and dolomite [146]. IR is considered a cost-effective and relatively accurate quantification method for carbonates, amorphous silica, and organic matter [147]. Recent studies are also looking at the quantification of clay minerals [148]. Complex IR spectra from heterogeneous samples, such as SPM and sediments, can be further analyzed by multivariate curve resolution alternating least squares (MCR-ALS) [149,150]. This decomposes the IR spectra into multiple components and computes their respective percentage [151,152]. As such, the change or evolution of SPM components can be followed along a river course or as a function of variable river flow. Furthermore, the same approach can be used to detect even minute IR changes that would not be possible without any treatment [153]. Ref. [143] used NIR spectroscopy on twenty-nine SPM samples in a 1.19 km^2 watershed in Brazil. They were able to differentiate the sources of the SPM using this technique. In their study, ref. [154] used FTIR to investigate the variations in the SPM mineral and organic composition. They found that SPM samples were mainly composed of quartz (peaks at 696, 780, 800, 1018 and 1868 cm^{-1}) and carbonates (peaks at 713, 729, 874, 1457, 1794, 2517 and 2873 cm^{-1}) with

no large variations along the river course. Ref. [142] used DRIFT spectroscopy to evaluate the efficiency of this technique in tracing sediment sources. They analyzed 50 samples from a small catchment (90 ha) in France and showed that this technique can separate at least four different sources from soil and river channel sediments. Ref. [143] compared classical geochemical and radionuclide tracers and a method using MIR spectroscopy to fingerprint sediments from rural catchments in Mexico. They found similar results except for one catchment due to the presence of high organic matter content. The use of VNIR spectroscopy was also successful for sediment fingerprinting in Ethiopia [155]. In particular cases, the use of spectroscopy methods cannot be used. For example, ref. [139] showed that Quaternary deposits in France could not be discriminated because the gypsum was not conservative.

In SPM studies, FTIR is commonly used in its bulk application, namely, the analysis of homogenized powders or bulk filter loads to obtain an average mineralogical and organic fingerprint (e.g., via DRIFT or ATR) [36,113]. Micro-FTIR (μFTIR) mapping of individual particles does exist; however, its application in riverine SPM studies seems to be absent. By contrast, micro-Raman spectroscopy (see Section 3.5.4) is almost exclusively deployed as a point-specific, single-particle technique to identify polymorphs (e.g., calcite vs. aragonite, iron oxides) and trace phases that are otherwise unresolvable by bulk FTIR or XRD [156]. The present division thus reflects the dominant operational use of each technique in the current SPM literature, rather than an inherent instrumental limitation.

3.4. Spatially Resolved Elemental and Mineral Mapping

3.4.1. Micro-X-Ray Fluorescence (μXRF)

Micro-X-ray fluorescence (μXRF) bridges bulk and particle-scale mineral characterization. It uses a focused (typically 10–50 μm) polychromatic or monochromatic X-ray beam [157]. Although rare in river SPM studies, it can be applied to SPM concentrated on filters, embedded in resin, or prepared as powder samples in XRF sample cups (in the presence of a few hundred mg of sample). μXRF provides semi-quantitative to quantitative elemental distribution maps that can reveal chemical heterogeneity, grain-scale elemental associations (e.g., Fe-(oxy)hydroxide coatings on clay minerals), and particle size-elemental composition relationships that bulk digestion-based ICP methods cannot resolve, at a much lower cost and analysis time than SEM-EDS mapping [158–160]. Its main limitations are a coarser spatial resolution than SEM-EDS or TEM, a detection sensitivity for light elements ($Z < 11$) that is generally poor compared with SEM-EDS, and a strong dependence of quantification accuracy on sample surface flatness and matrix effects, which are difficult to control for loosely packed filtered SPM. Open-access (e.g., Fiji/ImageJ) and commercial platforms (e.g., M4 TORNADO) are able to identify possible minerals and semi-quantify them based on elemental correlations [161]. Detailed information on automated mineralogy is discussed later (Section 3.5.1).

3.4.2. Laser Ablation ICP-MS (LA-ICP-MS)

Laser ablation ICP-MS (LA-ICP-MS) couples a pulsed laser, used to ablate a small volume (typically a few to tens of μm in diameter) directly from a solid sample, to an ICP-MS for multi-elemental and isotopic analysis. Applied to riverine SPM, LA-ICP-MS allows direct, spatially resolved analysis of individual particles or of SPM concentrated as a pellet or on a filter, without the acid digestion step required by solution-based ICP-MS. This removes a major source of the sample-preparation artefacts discussed above for bulk ICP analyses and additionally allows spatial or grain-scale elemental information to be retained [162,163]. This makes LA-ICP-MS particularly attractive for sediment and SPM fingerprinting studies, where preserving the elemental signature of individual detrital grains or filter sub-areas is

more informative than a homogenized bulk digestion [164,165]. Filter-based LA-ICP-MS protocols developed as a low-reagent, low-waste alternative to acid digestion illustrate this approach for suspended sediment fingerprinting. The "filter pellet" method developed by [162] demonstrated that quantitative multi-element data of sufficient quality for sediment fingerprinting can be obtained directly from filter-bound sediments without digestion, using a simple pellet preparation. Analogous filter-based, minimal-preparation elemental approaches have also been demonstrated using laser-induced breakdown spectroscopy (LIBS) directly on SPM-loaded filters, offering rapid multi-element screening at the expense of the quantification accuracy achievable by ICP-MS [166]. The main limitations of LA-ICP-MS for SPM are the need for matrix-matched calibration standards (rarely available for natural, heterogeneous SPM), potential elemental fractionation during ablation, and a spot size that, for the smallest SPM size fractions, may sample several particles simultaneously, limiting true single-particle resolution.

3.5. Particle- to Atomic-Scale Microscopy and Spectroscopy

3.5.1. Scanning Electron Microscopy: Manual Analysis and Automated Mineralogy (SEM-EDS)

Scanning electron microscopy coupled with energy-dispersive X-ray spectroscopy (SEM-EDS) is, together with manual optical microscopy, one of the most widely accessible tools for the particle-scale characterization of SPM, and arguably a workhorse technique of mineralogical SPM studies even though it is often only briefly mentioned in reviews of this kind. In its conventional, manual mode, individual particles deposited on a filter, stub, or polished mount are imaged under secondary-electron (topography) or backscattered-electron (mean atomic number contrast) detectors, and point or small-area EDS spectra are acquired manually on selected particles of interest [167,168]. This approach requires comparatively little sample preparation: particles can often be analyzed directly on the collection filter after conductive coating, and it makes minimal a priori assumptions about particle mineralogy. It delivers textural information (morphology, aggregation state, particle-particle associations) together with semi-quantitative elemental composition at the single-particle scale that cannot be retrieved from bulk methods (SSA, ICP, XRD, FTIR) alone [167,169]. Ref. [170] used SEM-EDS to investigate the structure and motion behavior of SPM in a slow-moving river in northern China, revealing how particle morphology and aggregation influence transport dynamics. Similarly, ref. [171] combined SEM-EDS with other techniques to demonstrate that SPM dynamics control mercury partitioning and transport in the Yellow River, highlighting the importance of particle-scale characterization for understanding contaminant behavior. Its main limitation is throughput; because particles are selected and analyzed one at a time by the operator, manual SEM-EDS is comparatively slow, poorly suited to statistically robust particle-population statistics, and susceptible to operator-selection bias, e.g., preferentially imaging visually distinctive particles. Nonetheless, it remains indispensable for targeted investigations, such as documenting specific contaminant-bearing phases, textures, or organo-mineral associations, and for validating the phase assignments made by automated systems.

Automated mineralogy (AM) systems address the throughput limitation of manual SEM-EDS by coupling automated stage control, backscattered-electron image segmentation, and EDS spectral acquisition and classification against a reference mineral database, allowing thousands of particles to be classified, sized, and their elemental associations quantified within a single, largely unattended session [172]. Commercial platforms (e.g., QEMSCAN, TIMA, Mineral Liberation Analyzer) were originally developed for ore characterization but are increasingly applied to environmental particles. Ref. [173], for instance, used SEM-based automated mineralogy (QEMSCAN) to distinguish natural sediments from iron ore tailings deposited in the Paraopeba River after the Brumadinho dam failure,

revealing six main mineral associations governed by different contents of quartz, kaolinite, and hematite. Similarly, automated mineralogy has been applied to distinguish geogenic from anthropogenic heavy metal sources in river and coastal sediments of the Jakarta Bay region [174]. These platforms are used in sediment samples more than SPM, at this stage, to provide modal mineralogy, particle-size and particle-shape distributions, and quantitative mineral-association statistics, for example, the proportion of Fe-oxide surface area in contact with phyllosilicates, that would be impractical to obtain manually [175–177]. Automated mineralogy nonetheless requires substantial sample preparation: particles are typically embedded in an epoxy resin mount, ground and polished to a flat, particle-representative cross-section, and carbon-coated [178,179]. This preparation is destructive and can introduce artefacts, including particle re-orientation, loss of the finest colloidal fraction, and cross-sectioning that alters the apparent size and shape of the original three-dimensional particle relative to a projected view [176,180]. It also requires from a few to several tens of milligrams of material, which can be limiting for low-concentration SPM samples. Phase assignment further relies on matching each measured EDS spectrum to a reference library. Poorly crystalline, mixed, or very fine-grained phases common in SPM (amorphous Fe/Al (oxy)hydroxides, clay-organic aggregates) are prone to misclassification or require bespoke reference libraries, and complementary XRD is generally recommended to validate the mineral phases assigned by AM [172].

3.5.2. Transmission Electron Microscopy

Several techniques allow characterization of the mineral composition at micro to nano scale. Transmission electron microscopy coupled with energy-dispersive spectroscopy (TEM-EDS), has been shown to be an extremely powerful tool for examining geochemical questions at the individual particle scale. TEM can assess the size, morphology, crystallinity, and elemental composition of single particles as well as determine their physical and spatial associations [181]. This technique can provide high-resolution imaging of thin samples with quantitative chemical analysis.

The classical preparation requires chemical stabilization, followed by sample dehydration and resin embedding, prior to ultramicrotomy. The multiple steps can lead to morphological artifacts such as aggregation of particles [182]. To avoid these morphological problems, resin impregnation is recommended [183]. A very easy preparation step used for SPM consists of re-suspending dried SPM in ethanol and laying down a drop on a cover grid [37]. TEM analysis is mainly used in SPM studies to investigate the morphology and nature of particles and the speciation of contaminants. Chemical analysis within the microscope can be obtained by energy-dispersive spectrometry (EDS) [184] or by electron energy loss spectrometry (EELS) [185]. EELS is more suitable for thin specimens (30–200 nm) [186]. Several mineral substances can be encountered in the literature [187,188]. Studies concerning aquatic particles using TEM as an analytical tool started in the late 1980's. Concerning oxic fresh waters, the inorganic fraction is mainly composed of aluminosilicates, silica, and iron oxyhydroxides [37,189]. Iron in SPM has been extensively investigated because of its important role in supplying nutrients to aquatic biota and its role as a sorbent. Natural anoxic waters have also been investigated. Especially the colloids composed of elemental sulfur and iron sulfide [190].

Beyond conventional TEM imaging, several complementary imaging and analytical modes provide different types of information and are not always clearly distinguished in previous SPM reviews. Scanning transmission electron microscopy (STEM) raster-scans a focused electron probe across the thin sample rather than illuminating it with a broad, parallel beam. When combined with EDS (STEM-EDS), it enables high-spatial-resolution elemental mapping, down to a few nanometers, of individual grains and organo-mineral in-

terfaces that is difficult to achieve in conventional TEM [191]. High-angle annular dark-field STEM (STEM-HAADF) collects electrons scattered to high angles, producing image contrast that scales approximately with the square of the atomic number (Z-contrast imaging) [192]. This makes STEM-HAADF particularly effective for visualizing heavy-element-bearing nanophases, e.g., Fe- or Pb-bearing nanoparticles, against a lighter aluminosilicate, clay mineral, or organic matrices.

Sample preparation for TEM/STEM is a major, and frequently under-discussed, source of artefacts in SPM studies. Even a single mineral grain or floc frequently requires the preparation of an ultrathin (<100 nm) section or lamella before analysis, obtained either by ultramicrotomy of a resin-embedded sample or, increasingly, by focused ion beam (FIB) milling. Ultramicrotomy can compress, tear, or redistribute soft organic and poorly consolidated mineral phases along the cutting direction [193]. It also necessarily exposes only a small, essentially random two-dimensional slice through a three-dimensional, often heterogeneous SPM aggregate, so the observed particle context, e.g., which mineral grains are in direct contact within a floc, may not be representative of the original aggregate architecture. FIB milling, in which a gallium (or increasingly plasma) ion beam cuts and thins a precisely targeted region of interest down to electron transparency, allows site-specific lamella extraction, for example targeting a contaminant hotspot identified by prior SEM-EDS or μXRF mapping, and better preserves the spatial relationships between phases. However, it can introduce Ga^{+} implantation, amorphization of the near-surface region, and local heating artefacts that must be considered when interpreting nanoscale structural or chemical data, particularly for beam-sensitive phases such as poorly crystalline Fe (oxy)hydroxides [194]. Both approaches remove the sample from its native aqueous environment and require some dehydration or resin embedding, which is itself a source of the aggregation and morphological artefacts noted above.

Cryogenic electron microscopy (cryo-EM), in which the hydrated sample is vitrified by rapid plunge-freezing rather than chemically fixed and dehydrated, largely avoids these dehydration- and embedding-related artefacts by preserving particles, aggregates, and their associated water and organic coatings in a near-native, frozen-hydrated state [195]. Although cryo-EM has been most extensively developed for structural biology and synthetic colloidal nanoparticles, its extension to environmental and geological materials is a rapidly growing area of clear relevance to SPM, particularly for imaging fragile organo-mineral flocs, biofilm-mineral associations, and poorly crystalline nanophases that are otherwise altered or destroyed by conventional preparation [195]. A complementary, still largely exploratory avenue is in-situ (liquid-cell) TEM, in which particles are imaged directly within a thin layer of liquid enclosed between electron-transparent membranes, allowing dynamic processes such as aggregation, dissolution, or nanoparticle nucleation to be observed in real time [196]. Its application to natural, compositionally complex SPM remains limited by electron-beam-induced radiolysis of the liquid and by the difficulty of preserving representative aggregate structures within the confined liquid cell. It nonetheless represents a promising direction for directly capturing the dynamic behavior of SPM that static, ex-situ TEM cannot access.

3.5.3. Atomic Force Microscopy (AFM)

Atomic force microscopy (AFM), in contrast to conventional SEM and TEM, can distinguish between grains and aggregates [197]. Quite new techniques known as scanning probe microscopy permit direct imaging of particles with very high resolution (up to atomic). Different techniques are available, including atomic force microscopy (AFM), magnetic force microscopy (MFM), electrostatic force microscopy (EFM), lateral force microscopy (LFM), electrochemical atomic force microscopy (ECAFM) [198]. These techniques are

very promising for exploring SPM surfaces, visualizing the sorption of organic substances, determining the morphology, and measuring size and thickness [199]. Several studies characterized the morphology of pure minerals forming SPM, such as illite, smectite, iron oxides, and calcite [200–202].

AFM is by far the most common SPM technique to probe natural SPM. AFM has a high spatial resolution and can image samples in different environments [203].

The studies are generally performed under ambient air conditions. Such preparation may result in artefacts. AFM is a high-resolution surface imaging tool, extremely powerful for the determination of colloidal topography/height on the basis of the repulsive or attractive forces between the sample and the tip [204]. The AFM can be operated in air or in fluid [205]. More than 10 different imaging modes can be used in AFM analysis [206], yet three are commonly encountered in AFM imaging: contact, tapping, and non-contact modes. In contact mode, the tip is in contact with the sample all the time. This mode is associated with high shear forces and can damage samples. In non-contact mode, the tip oscillates at a frequency slightly higher than its resonance frequency, several nanometers above the sample. In tapping mode, the cantilever oscillates near its resonance frequency at an amplitude ranging from 100 to 200 nm and touches the sample [207]. Different sample preparations can be used, such as particle sorption to a freshly cleaved flat surface, drop deposition, and particle ultracentrifugation [208].

Ref. [203] investigated the effects of the analysis mode (contact vs. non-contact modes) as well as the analysis environment (liquid vs. ambient air) and sample preparation. They found that the non-contact mode was the most appropriate for the characterization of natural colloids. In addition, the lack of washing after adsorption or sample preparation by drop deposition can result in the formation of aggregation and salt crystallization. Finally, they found that liquid-mode imaging is not necessary for size measurement if minimally perturbing sample preparation is employed. Ref. [209] used AFM in tapping mode to study the size distribution, surface coverage, and morphology of aquatic colloids. They found three types of natural aquatic colloids based on their shape and size. Ref. [210] successfully used AFM to study the surface area and reactivity of several phyllosilicates (kaolinite, hectorite, and nontronite). Other studies on phyllosilicates were also extended to illite and montmorillonite [211], smectite [200], mica and muscovite [212,213], oxides [201], calcite [202], goethite [214], and hematite [215].

3.5.4. Raman Spectroscopy

While Section 3.3.2 described FTIR as a bulk vibrational method, the complementary vibrational technique, micro-Raman spectroscopy, is discussed here because its conventional application to SPM involves point-specific analysis of individual particles rather than bulk homogenized powders.

Raman spectroscopy is a vibrational spectroscopic technique, complementary to infrared spectroscopy, based on the inelastic (Raman) scattering of monochromatic laser light by molecular and lattice vibrations, which produces a spectrum of characteristic bands that can act as a mineral- and, in favorable cases polymorph-, polymorph-specific fingerprint [216]. Coupled with an optical or confocal microscope (micro-Raman), it allows essentially preparation-free, non-destructive analysis of individual SPM particles at approximately 1 µm spatial resolution, without the coating, embedding, or vacuum required by SEM-EDS or TEM, which is a substantial practical advantage for rapid particle screening. Micro-Raman is particularly well suited to distinguishing mineral polymorphs that share an identical elemental composition and are therefore indistinguishable by EDS alone, for example anatase, rutile, and brookite among TiO_2 polymorphs, calcite versus aragonite, or the different iron oxide/oxyhydroxide phases such as goethite, hematite, and ferrihy-

drite [217], and it can identify organic and microplastic components intermixed with the mineral fraction of SPM within the same analytical session. In practice, Raman spectroscopy is often combined with other techniques to obtain a comprehensive picture of nanoparticle geochemistry, as demonstrated by [218], who used field emission SEM, HR-TEM, and selected area electron diffraction alongside EDS to characterize nanoparticles (<100 nm) in suspended sediments from the Magdalena River, identifying Al, Ti, and Fe oxides as well as other elements. The main Raman spectroscopy limitations for SPM characterization are threefold. First, some clay minerals and organic-coated particles produce a fluorescence background that can mask the Raman signal, giving comparatively low sensitivity for several environmentally important, weakly Raman-active or strongly fluorescent phases. Second, spectra are acquired point-by-point, so true bulk quantification is not possible: mineral proportions must be inferred from many individual particle analyses rather than measured directly as in XRD. Third, laser power must be carefully controlled to avoid heating or phase transformation of fragile or strongly light-absorbing particles.

3.5.5. X-Ray Absorption Fine Structure Spectroscopy

Extended X-ray Absorption Fine Structure (EXAFS) spectroscopy started in the 1920s but gained widespread recognition in the mid-1970s following the advent of synchrotron radiation sources [46]. EXAFS was first applied to mineralogical studies in the 1980s [46,219], and the subsequent development of second- and third-generation synchrotron facilities greatly expanded its applicability to highly diluted environmental matrices such as SPM.

EXAFS is an element-specific spectroscopic technique that can be performed in two modes: (i) the Transmission mode, determined by measuring the intensity of the X-ray beam passing through the sample (suited for concentrated samples) and (ii) the Fluorescence mode, determined by measuring the secondary X-ray fluorescence emitted by the target element (for diluted samples).

Beyond the absorption edge, interference between the outgoing photoelectron wave emitted by the absorbing atom and the waves backscattered by surrounding neighboring atoms generates oscillations in the absorption coefficient. EXAFS provides precise insights into the local chemical and structural environment around the absorber up to a distance of approximately 5–6 Å. This allows for the determination of the coordination number, the chemical identity of neighboring atoms, interatomic distances, and the degree of structural order or disorder within the coordination shells [43,220].

To extract structural information from EXAFS oscillations, two primary analytical approaches are employed: (i) linear combination fitting and (ii) numerical simulation and shell fitting.

Linear combination fitting provides an estimation of the local atomic environment without the immediate need for complex numerical simulations. Using a least-squares minimization protocol, the experimental spectrum is modeled as a linear combination of reference spectra obtained from well-characterized standard compounds. The contribution of each reference component is directly proportional to its fractional abundance within the sample. To maintain physical relevance and avoid overfitting, the decomposition of the experimental spectrum is typically restricted to a maximum of three or four reference compounds. While the sum of all components ideally equals 100%, lower sums (e.g., ~70%) can yield acceptable fits in specific diluted or complex systems. This approach serves as an efficient tool for phase identification, despite carrying a structural uncertainty of approximately 10% to 15%. This approach is routinely used for SPM studies. Ref. [221] investigated the speciation of Zn in SPM from the Seine River (France). The results showed, using LCF, significant spatial variations in Zn speciation along the river continuum. Upstream of Paris, Zn was mainly associated with calcite, either adsorbed onto its surface or incorporated

into its crystal structure. In contrast, downstream of Paris, amorphous zinc sulfide (ZnS) became the dominant Zn-bearing phase, reflecting the influence of anthropogenic inputs from the Paris metropolitan area. A similar study was conducted for Zn speciation in one affluent of the Seine River (Orge River). Coupled with TEM and SEM analyses, this study showed that Zn speciation depended not only on urbanization but also on River flow rate [189]. Another study [222] used an EXAFS approach coupled with isotopy (see below paragraph) to investigate the influence of land use on trace metal dynamics in three contrasting sub-basins of the Seine River watershed. Results showed significant anthropogenic impacts on both dissolved and particulate fractions, with distinct sources depending on land use. Zinc speciation, isotopic signatures, and export rates further highlighted the role of forested, agricultural, and urban areas in controlling trace metal transport and cycling.

Numerical simulation and shell fitting, by contrast, provide a highly precise determination of structural parameters through a complementary route. The resulting partial spectrum is subsequently fitted in both frequency and amplitude using a theoretical approach based on the standard EXAFS equation under the single-scattering approximation. The adjustable parameters are categorized into two groups: (i) the structural parameters (the coordination number of neighboring atoms (Ni), the Debye-Waller factor (σi, reflecting structural and thermal disorder), the photoelectron mean free path (λi = k/Γi), the interatomic distance (Ri), and the energy threshold shift (ΔE0) between the experimental edge and the theoretical value) (ii) the electronic parameters (the element-specific amplitude (A(k)) and phase shift (Φ(k)) functions for each atomic pair, alongside the amplitude reduction factor (S02, often fixed to 1). These electronic functions are theoretically calculated using ab initio codes such as FEFF and validated against reference compounds with known crystal structures. This numerical optimization yields highly precise structural data, with typical uncertainties of approximately ±0.02 Å for interatomic distances (Ri) and ±20% for coordination numbers (Ni). This approach was first used for single minerals. Documented examples include Zn adsorption on clay minerals [223], montmorillonite [224,225], smectite [226], calcite [227], and ferrihydrite [35]. Some studies also used this approach for SPM. Ref. [31] monitored changes in mineralogy and composition of authigenic material from its source to streams of increasing order. EXAFS analyses revealed that freshly precipitated Fe-rich particles formed from groundwater oxidation consisted mainly of poorly crystalline hydrous ferric oxides with a structure similar to ferrihydrite. The Fe speciation remained largely unchanged during downstream transport, although an increase in Fe–Fe interactions indicated progressive ageing and hydrolysis of the ferrihydrite-like phases. Ref. [228] also tried this approach to better understand the Zn speciation in SPM from the Moselle River (North East of France). They conducted Zn adsorption tests on natural SPM and observed that at low Zn loadings, the binding mode of Zn with SPM was controlled by its own mineral composition.

3.6. Critical Synthesis and Comparison of Analytical Approaches

The previous sections described, technique by technique, the mineral information that can be obtained from riverine SPM. Existing reviews and textbook descriptions of SPM characterization, including many of the foundational works cited throughout this article, have generally been structured in this same technique-by-technique manner, treating individual methods (e.g., ICP-MS, XRD, and TEM) as largely self-contained topics. These treatments provide limited explicit discussion of how the sample preparation choices, detection limits, and spatial or particle size resolution of a given method constrain the environmental interpretations that can be drawn from it, and they offer correspondingly little guidance on how methods should be combined for a given research question. This descriptive, method-centered structure is a genuine limitation of the existing literature. For

riverine SPM, arguably more than for many other geological materials, no single technique can characterize the full range of particle sizes (colloidal to >100 µm), mineralogical states (from well-crystalline detrital grains to amorphous authigenic coatings), and spatial scales (bulk sample to individual nanoparticle) relevant to its environmental reactivity. Table 1 therefore synthesizes, across all methods discussed in this review, the sample requirement, the spatial or particle-size resolution achieved, the type of information provided, the principal sample-preparation artefacts, and the methods most usefully combined with each technique, to support method selection and result interpretation rather than provide a simple inventory of available instrumentation.

Table 1. Comparative synthesis of the sampling and analytical methods discussed in this review for the mineralogical characterization of riverine SPM.

Method	Sample Requirement	Spatial/Particle-Size Resolution	Information Provided	Main Preparation Artefacts	Best Complementary Method(s)
SSA (BET, EGME)	mg-g, dried/degassed	Bulk (no spatial resolution)	Surface area, micro-/mesoporosity	Outgassing can alter Fe-oxides; removes bound water	ICP-MS/OES, XRD
ICP-MS/OES	~1 g (fusion) or mg (digestion)	Bulk	Elemental concentrations (ppt-ppm)	Partial vs. total digestion; contamination	XRD, isotope MS
XRD	tens-hundreds mg	Bulk (mm-scale beam)	Crystalline minerals and quantification	Preferred orientation; amorphous phases need internal standard	FTIR, automated mineralogy
FTIR	A few mg	Bulk	Mineral + organic functional groups	Overlapping bands in mixtures	XRD, MCR-ALS
µXRF	Filter/mount; no digestion	10–50 µm	2D elemental maps	Surface flatness and matrix effects	SEM-EDS, XRD
LA-ICP-MS	Few mg or individual grains	~10–50 µm spot	Spatially resolved multi-element/isotope data	Matrix-matched standards; ablation fractionation	SEM-EDS, automated mineralogy
SEM-EDS (manual)	Individual particles	~1 µm (nm with FEG)	Morphology + semi-quantitative elemental composition	Coating; operator selection bias	XRD, TEM
Automated mineralogy (SEM-AM)	mg, polished mount	~1 µm; 1000 s of particles	Modal mineralogy, particle size/shape, associations	Polishing/embedding; EDS-library misclassification	XRD, manual SEM-EDS
TEM/STEM-EDS/STEM-HAADF	ng-µg, ultrathin section	nm–Å	Morphology, crystallinity, elemental or Z-contrast at particle scale	Ultramicrotomy/FIB artefacts; dehydration	EXAFS, SEM-EDS
Cryo-EM/in-situ (liquid-cell) TEM	ng-µg, vitrified or in liquid cell	nm	Native-state morphology; dynamic processes	Vitrification quality; beam-induced radiolysis	Conventional TEM
AFM	Individual particles, deposited/dried	nm (height); atomic (lattice)	Topography, height, aggregation state	Ambient drying; tip-sample interaction	TEM, SEM-EDS
Micro-Raman	Individual particles; no prep	~1 µm	Mineral/polymorph fingerprint	Fluorescence background; laser-induced damage	SEM-EDS, XRD
EXAFS/XAS	mg (diluted) to individual grains	Local atomic environment (element-specific)	Speciation, coordination, oxidation state	Beam damage; LCF reference-set bias	TEM, isotope MS
Isotope ratio MS (MC-ICP-MS)	mg, chemically purified	Bulk (per separated fraction)	Source tracing, process fractionation	Cleanroom digestion/purification; contamination	ICP-MS, EXAFS

BET: Brunauer-Emmett-Teller; EGME: ethylene glycol monomethyl ether; MCR-ALS: multivariate curve resolution-alternating least squares; FEG: field-emission gun; FIB: focused ion beam; LCF: linear combination fitting.

Several general patterns emerge from this synthesis. First, resolution and representativeness are generally traded off against one another. Bulk techniques (SSA, ICP-MS/OES, XRD, FTIR) analyze statistically representative sample masses but average over highly heterogeneous particle populations, whereas particle-scale techniques (SEM-EDS, automated mineralogy, TEM/STEM, AFM, micro-Raman) resolve individual particles or small assemblages but analyze only a minute, potentially non-representative fraction of the total sample unless very large numbers of particles are measured, as in automated mineralogy. Second, virtually every technique requires some form of sample preparation, such as drying, grinding, digestion, embedding, polishing, coating, or dehydration, that can itself alter the property being measured. The resulting artefacts differ systematically between methods (e.g., digestion artefacts for ICP-MS versus embedding artefacts for TEM/automated mineralogy versus filtration artefacts common to nearly all techniques). No technique in Table 1 is artefact-free, and results should always be interpreted with the relevant preparation step in mind. Third, methods that provide chemical/elemental information (ICP-MS/OES, μXRF, LA-ICP-MS, EDS) are rarely, by themselves, diagnostic of mineral phase, whereas methods that are phase-diagnostic (XRD, Raman, EXAFS) generally provide lower spatial resolution or lower sensitivity for trace and poorly crystalline phases. Combining a phase-diagnostic and an elemental/chemical technique is therefore almost always necessary to unambiguously identify and quantify a mineral phase of interest in SPM. These considerations, rather than a simple listing of instrumentation, are what should guide method selection in future SPM studies, and they underline why no single analytical technique, however powerful, can replace a multi-scale, multi-technique approach for characterizing the mineral fraction of natural SPM.

3.7. Emerging Perspectives: Artificial Intelligence, Machine Learning, and Multimodal Data Fusion

A further limitation of the existing SPM characterization literature is the near-absence of any discussion of artificial intelligence (AI), machine learning (ML), and multimodal data fusion, even though these approaches are being rapidly adopted across mineralogical and geochemical disciplines more broadly [229]. In automated mineralogy and SEM/TEM imaging, machine-learning-based image segmentation and classification algorithms are increasingly used to replace or supplement traditional EDS spectral-matching against reference libraries, improving the identification of poorly crystalline or compositionally intermediate phases that are common in SPM and problematic for simple look-up-table classification [230,231]. In vibrational spectroscopy, supervised classification and spectral unmixing algorithms (building on approaches such as MCR-ALS already used for FTIR, see Section 3.3.2) are being extended to automatically decompose complex Raman and infrared spectra of heterogeneous natural samples into their constituent mineral and organic end-members with less operator intervention than classical peak-fitting approaches [232,233].

Perhaps the greatest potential for SPM research lies in multimodal data fusion, the combination of data from several of the techniques discussed above (e.g., SEM-EDS particle maps, μXRF elemental maps, XRD bulk mineralogy, and hydrological/physicochemical parameters) into a single predictive or classification framework, rather than the sequential, largely qualitative cross-referencing of separate datasets that is current practice in most SPM studies. Fusion can occur at the raw-data level, at an intermediate feature level, or at the level of the final classification/decision from each modality, each with different trade-offs between information preservation and robustness to missing or noisy modalities, an important practical consideration for field-collected SPM datasets, which are frequently incomplete for at least one variable or sampling date [229]. Such approaches remain largely unexplored for riverine SPM specifically. They have, however, already demonstrated value in adjacent fields, including automated mineral identification, mineral prospectivity predic-

tion from heterogeneous geoscience data, and the fusion of complementary spectroscopic techniques (e.g., LIBS and Raman) for mineral identification, and represent a promising, currently underexploited, direction for integrating the multi-technique, multi-scale datasets that this review shows are necessary to fully characterize the mineral fraction of natural SPM. The benefits of such multimodal approaches have already been demonstrated in adjacent mineralogical and geochemical applications. For example, the combination of Raman spectroscopy and laser-induced breakdown spectroscopy (LIBS) has been shown to improve mineral identification compared with either technique used independently, with mid-level data fusion providing a direct example of the advantages of integrating complementary spectroscopic information [234]. Similarly, the fusion of LIBS and Raman data with machine-learning classifiers has achieved high mineral-identification accuracy, demonstrating that the complementary chemical and molecular information provided by the two techniques can be exploited within a unified analytical framework [235].

4. Conclusions

Suspended particulate matter (SPM) is a fundamental component of riverine ecosystems, from headwaters to estuaries, and plays a central role in the transport of sediments, nutrients, contaminants, and trace metals. Understanding its spatial and temporal dynamics is therefore essential for improving our knowledge of biogeochemical processes and for assessing the environmental impacts of natural and anthropogenic pressures.

This review critically compared the principal sampling strategies and analytical techniques available for characterizing the mineral fraction of riverine SPM, from bulk approaches (specific surface area, elemental and mineralogical analyses) to particle- and atomic-scale methods (manual and automated electron microscopy, atomic force microscopy, X-ray absorption spectroscopy, isotopic analyses). It synthesizes their sample requirements, spatial resolution, preparation artefacts, and complementarity in a single comparative table (Table 1). No single analytical method is sufficient to fully characterize the mineral fraction of natural SPM. Each technique trades off representativeness against spatial resolution and carries its own preparation artefacts. As a result, a multi-scale, multi-technique approach, guided by the specific research question rather than by instrument availability, is required to obtain a robust understanding of particle composition, structure, reactivity, and contaminant associations. Future progress will depend on three complementary developments. First, the standardization of sampling procedures and sample-preparation protocols, together with international databases dedicated to SPM mineralogical, chemical, and physical characteristics, similar to critical zone observatories, would considerably improve comparability between studies conducted in different river systems worldwide. Second, in-situ and autonomous sampling and sensing technologies, together with cryogenic and in-situ electron microscopy, offer growing opportunities to capture the short-term variability and native-state structure of SPM that discrete, ex-situ sampling and conventional preparation cannot resolve. Third, machine-learning-based classification and multimodal data fusion, combining several of the techniques reviewed here into unified predictive frameworks, represent a largely untapped opportunity to move beyond the sequential, qualitative cross-referencing of separate datasets that still characterizes most current SPM studies. Combined with advanced laboratory experiments and field observations, these developments should improve our understanding of SPM processes under changing environmental conditions.

Author Contributions: Conceptualization, M.L.M.; investigation, M.L.M., P.L.V., A.H.N. and H.J.K.; data curation, M.L.M. and H.J.K.; writing—original draft preparation, M.L.M., P.L.V., A.H.N. and H.J.K.; writing—review and editing, M.L.M. and H.J.K.; visualization, M.L.M. and H.J.K.; supervision, M.L.M. All authors have read and agreed to the published version of the manuscript.

Funding: This research received no external funding.

Data Availability Statement: No new data were created or analyzed in this study. Data sharing is not applicable to this article.

Conflicts of Interest: The authors declare no conflict of interest.

References

1. Stumm, W.; Morgan, J.J. *Aquatic Chemistry: Chemical Equilibria and Rates in Natural Waters*; John Wiley & Sons: Hoboken, NJ, USA, 2013.
2. Eisma, D. *Suspended Matter in the Aquatic Environment*; Springer: Berlin/Heidelberg, Germany, 1993.
3. Droppo, I.G. Rethinking What Constitutes Suspended Sediment. *Hydrol. Process.* **2001**, *15*, 1551–1564. [CrossRef]
4. Henning, K.H.; Damke, H.; Kasbohm, J.; Puff, T.; Breitenbach, E.; Theel, O.; Kießling, A. *Schwebstoffbeschaffenheit Im Odersystem*; Ernst-Moritz-Arndt-Universität Greifswald: Greifswald, Germany, 2001.
5. Zimmermann-Timm, H. Characteristics, Dynamics and Importance of Aggregates in Rivers—An Invited Review. *Int. Rev. Hydrobiol.* **2002**, *87*, 197–240. [CrossRef]
6. Walch, H.; von der Kammer, F.; Hofmann, T. Freshwater Suspended Particulate Matter—Key Components and Processes in Floc Formation and Dynamics. *Water Res.* **2022**, *220*, 118655. [CrossRef] [PubMed]
7. Ho, Q.N.; Fettweis, M.; Spencer, K.L.; Lee, B.J. Flocculation with Heterogeneous Composition in Water Environments: A Review. *Water Res.* **2022**, *213*, 118147. [CrossRef] [PubMed]
8. Lee, B.J.; Fettweis, M.; Toorman, E.; Molz, F.J. Multimodality of a Particle Size Distribution of Cohesive Suspended Particulate Matters in a Coastal Zone. *J. Geophys. Res. Ocean.* **2012**, *117*, C03014. [CrossRef]
9. Collins, A.L.; Walling, D.E.; Leeks, G.J.L. *Storage of Fine-Grained Sediment and Associated Contaminants within the Channels of Lowland Permeable Catchments in the UK*; IAHS Press: Wallingford, UK, 2005; pp. 259–269.
10. Quinton, J.N.; Govers, G.; Van Oost, K.; Bardgett, R.D. The Impact of Agricultural Soil Erosion on Biogeochemical Cycling. *Nat. Geosci.* **2010**, *3*, 311–314. [CrossRef]
11. Walling, D.E.; Collins, A.L. Fine Sediment Transport and Management. In *River Science: Research and Management for the 21st Century*; Gilvear, D.J., Greenwood, M.T., Thoms, M.C., Wood, P.J., Eds.; John Wiley & Sons, Ltd.: Chichester, UK, 2016; pp. 37–60.
12. Walling, D.E. Human Impact on Land–Ocean Sediment Transfer by the World's Rivers. *Geomorphology* **2006**, *79*, 192–216. [CrossRef]
13. Frings, R.M.; Ten Brinke, W.B.M. Ten Reasons to Set up Sediment Budgets for River Management. *Int. J. River Basin Manag.* **2018**, *16*, 35–40. [CrossRef]
14. Grimardias, D.; Guillard, J.; Cattanéo, F. Drawdown Flushing of a Hydroelectric Reservoir on the Rhône River: Impacts on the Fish Community and Implications for the Sediment Management. *J. Environ. Manag.* **2017**, *197*, 239–249. [CrossRef] [PubMed]
15. Owens, P.N.; Batalla, R.J.; Collins, A.J.; Gomez, B.; Hicks, D.M.; Horowitz, A.J.; Kondolf, G.M.; Marden, M.; Page, M.J.; Peacock, D.H.; et al. Fine-Grained Sediment in River Systems: Environmental Significance and Management Issues. *River Res. Appl.* **2005**, *21*, 693–717. [CrossRef]
16. Dumas, C.; Ludwig, W.; Aubert, D.; Eyrolle, F.; Raimbault, P.; Gueneugues, A.; Sotin, C. Riverine Transfer of Anthropogenic and Natural Trace Metals to the Gulf of Lions (NW Mediterranean Sea). *Appl. Geochem.* **2015**, *58*, 14–25. [CrossRef]
17. Evrard, O.; Laceby, J.P.; Lepage, H.; Onda, Y.; Cerdan, O.; Ayrault, S. Radiocesium Transfer from Hillslopes to the Pacific Ocean after the Fukushima Nuclear Power Plant Accident: A Review. *J. Environ. Radioact.* **2015**, *148*, 92–110. [CrossRef] [PubMed]
18. Horowitz, A.J. Determining Annual Suspended Sediment and Sediment-Associated Trace Element and Nutrient Fluxes. *Sci. Total Environ.* **2008**, *400*, 315–343. [CrossRef] [PubMed]
19. Viers, J.; Dupré, B.; Gaillardet, J. Chemical Composition of Suspended Sediments in World Rivers: New Insights from a New Database. *Sci. Total Environ.* **2009**, *407*, 853–868. [CrossRef] [PubMed]
20. Walling, D.E.; Fang, D. Recent Trends in the Suspended Sediment Loads of the World's Rivers. *Glob. Planet. Change* **2003**, *39*, 111–126. [CrossRef]
21. Négrel, P.; Grosbois, C. Changes in Chemical and $^{87}Sr/^{86}Sr$ Signature Distribution Patterns of Suspended Matter and Bed Sediments in the Upper Loire River Basin (France). *Chem. Geol.* **1999**, *156*, 231–249. [CrossRef]
22. Olivié-Lauquet, G.; Allard, T.; Bertaux, J.; Muller, J.-P. Crystal Chemistry of Suspended Matter in a Tropical Hydrosystem, Nyong Basin (Cameroon, Africa). *Chem. Geol.* **2000**, *170*, 113–131. [CrossRef]
23. Gaillardet, J.; Dupré, B.; Allègre, C.J. Geochemistry of Large River Suspended Sediments: Silicate Weathering or Recycling Tracer? *Geochim. Cosmochim. Acta* **1999**, *63*, 4037–4051. [CrossRef]
24. Buffle, J.; Leppard, G.G. Characterization of Aquatic Colloids and Macromolecules. 2. Key Role of Physical Structures on Analytical Results. *Environ. Sci. Technol.* **1995**, *29*, 2176–2184. [CrossRef] [PubMed]

25. Leppard, G.G.; Flannigan, D.T.; Mavrocordatos, D.; Marvin, C.H.; Bryant, D.W.; McCarry, B.E. Binding of Polycyclic Aromatic Hydrocarbons by Size Classes of Particulate in Hamilton Harbor Water. *Environ. Sci. Technol.* **1998**, *32*, 3633–3639. [CrossRef]
26. Montarges-Pelletier, E.; Jeanneau, L.; Faure, P.; Bihannic, I.; Barres, O.; Lartiges, B.S. The Junction of Fensch and Moselle Rivers, France; Mineralogy and Composition of River Materials. *Environ. Geol.* **2007**, *53*, 85–102. [CrossRef]
27. Eidam, J.; Lehmann, J.; Puff, T. *Einfluß Des Phasenbestandes von Schwebstoffen und Sedimenten Des Odermündungsgebietes Auf Die Bindung und Mobilisierung von Schwermetallen—Beitrag Zur Bilanzierung von Stoffaustauschprozessen*; Institut für Geologische Wissenschaften, Ernst-Moritz-Arndt-Universität Greifswald: Greifswald, Germany, 1997.
28. Slomberg, D.L.; Ollivier, P.; Radakovitch, O.; Baran, N.; Sani-Kast, N.; Miche, H.; Borschneck, D.; Grauby, O.; Bruchet, A.; Scheringer, M.; et al. Characterisation of Suspended Particulate Matter in the Rhone River: Insights into Analogue Selection. *Environ. Chem.* **2016**, *13*, 804–815. [CrossRef]
29. D'Sa, E.J.; Joshi, I.D.; Osburn, C.L.; Liu, B. Suspended Particulate Matter Distribution, Composition and Size Characteristics in Two Coastal Estuaries (Gulf of Mexico): Seasonal Variability and Influence on Hyperspectral Reflectance Signatures. *Sci. Total Environ.* **2025**, *987*, 179801. [CrossRef] [PubMed]
30. Poulton, S.W.; Raiswell, R. Chemical and Physical Characteristics of Iron Oxides in Riverine and Glacial Meltwater Sediments. *Chem. Geol.* **2005**, *218*, 203–221. [CrossRef]
31. Le Meur, M.; Montarges-Pelletier, E.; Gley, R.; Briois, V.; Michot, L.; Kanbar, H.; Caillet, C.; Razafitianamaharavo, A.; Villieras, F. Natural Suspended Particulate Matter (SPM) versus Lab-Controlled Particles: Comparison of the Reactivity and Association Mode of Zn. *Appl. Geochem.* **2022**, *140*, 105286. [CrossRef]
32. Atteia, O.; Perret, D.; Adatte, T.; Kozel, R.; Rossi, P. Characterization of Natural Colloids from a River and Spring in a Karstic Basin. *Environ. Geol.* **1998**, *34*, 257–269. [CrossRef]
33. Hirst, C.; Andersson, P.S.; Shaw, S.; Burke, I.T.; Kutscher, L.; Murphy, M.J.; Maximov, T.; Pokrovsky, O.S.; Mörth, C.-M.; Porcelli, D. Characterisation of Fe-Bearing Particles and Colloids in the Lena River Basin, NE Russia. *Geochim. Cosmochim. Acta* **2017**, *213*, 553–573. [CrossRef]
34. Neubauer, E.; Köhler, S.J.; von der Kammer, F.; Laudon, H.; Hofmann, T. Effect of PH and Stream Order on Iron and Arsenic Speciation in Boreal Catchments. *Environ. Sci. Technol.* **2013**, *47*, 7120–7128. [CrossRef] [PubMed]
35. Baken, S.; Sjöstedt, C.; Gustafsson, J.P.; Seuntjens, P.; Desmet, N.; De Schutter, J.; Smolders, E. Characterisation of Hydrous Ferric Oxides Derived from Iron-Rich Groundwaters and Their Contribution to the Suspended Sediment of Streams. *Appl. Geochem.* **2013**, *39*, 59–68. [CrossRef]
36. Kravchishina, M.D.; Dara, O.M. Mineral Composition of the Suspended Particulate Matter in the White Sea. *Oceanology* **2014**, *54*, 327–337. [CrossRef]
37. Le Meur, M.; Montarges-Pelletier, E.; Bauer, A.; Gley, R.; Migot, S.; Barres, O.; Delus, C.; Villiéras, F. Characterization of Suspended Particulate Matter in the Moselle River (Lorraine, France): Evolution along the Course of the River and in Different Hydrologic Regimes. *J. Soils Sediments* **2016**, *16*, 1625–1642. [CrossRef]
38. Mao, C.; Chen, J.; Yuan, X.; Yang, Z.; Balsam, W.; Ji, J. Seasonal Variation in the Mineralogy of the Suspended Particulate Matter of the Lower Changjiang River at Nanjing, China. *Clays Clay Miner.* **2010**, *58*, 691–706. [CrossRef]
39. Röttgers, R.; Dupouy, C.; Taylor, B.B.; Bracher, A.; Woźniak, S.B. Mass-specific Light Absorption Coefficients of Natural Aquatic Particles in the Near-infrared Spectral Region. *Limnol. Oceanogr.* **2014**, *59*, 1449–1460. [CrossRef]
40. Yao, C.; Dai, Z.; Shen, Z.; Tian, S.; Zhu, S.; Shi, J.; Xiang, Y.; Wang, Y.; Zhu, B.; Wang, D. Heavy Metal Speciation and Risk Assessment in Suspended Particulate Matter: A Case Study of Small-Medium Freshwater Bodies in Southwestern China. *J. Hazard. Mater.* **2026**, *501*, 140851. [CrossRef] [PubMed]
41. Ali, A.; Chiang, Y.W.; Santos, R.M. X-Ray Diffraction Techniques for Mineral Characterization: A Review for Engineers of the Fundamentals, Applications, and Research Directions. *Minerals* **2022**, *12*, 205. [CrossRef]
42. Pappas, N. Calculating Retained Austenite in Steel Post Magnetic Processing Using X-Ray Diffraction. *BS Undergr. Maths. Exch.* **2006**, *4*, 8–14.
43. Koningsberger, D.C.; Prins, R. *X-Ray Absorption: Principles, Applications, Techniques of EXAFS, SEXAFS and XANES*; John Wiley & Sons: Hoboken, NJ, USA, 1988.
44. Huynh, T.T.; Kim, J.; Lee, S.D.; Fettweis, M.; Bi, Q.; Kim, S.; Lee, S.; Choi, Y.Y.; Nguyen, H.S.; Bui, T.V.; et al. Spatiotemporal Dynamics of Suspended Particulate Matter in Water Environments: A Review. *Water* **2024**, *16*, 3613. [CrossRef]
45. Sharma, I. ICP-OES: An Advance Tool in Biological Research. *Open J. Environ. Biol.* **2020**, *5*, 27–33. [CrossRef]
46. Brown, G.E.; Calas, G.; Waychunas, G.A.; Petiau, J. X-Ray Absorption Spectroscopy; Applications in Mineralogy and Geochemistry. *Rev. Mineral. Geochem.* **1988**, *18*, 431–512. [CrossRef]
47. Aggarwal, J.; Habicht-Mauche, J.; Juarez, C. Application of Heavy Stable Isotopes in Forensic Isotope Geochemistry: A Review. *Appl. Geochem.* **2008**, *23*, 2658–2666. [CrossRef]
48. Mahler, B.J.; Van Metre, P.C. A Simplified Approach for Monitoring Hydrophobic Organic Contaminants Associated with Suspended Sediment: Methodology and Applications. *Arch. Environ. Contam. Toxicol.* **2003**, *44*, 288–297. [CrossRef] [PubMed]

49. Horowitz, A.J. Comparison of Methods for the Concentration of Suspended Sediment in River Water for Subsequent Chemical Analysis. *Environ. Sci. Technol.* **1986**, *20*, 155–160. [CrossRef] [PubMed]
50. Schäfer, J.; Blanc, G. Relationship between Ore Deposits in River Catchments and Geochemistry of Suspended Particulate Matter from Six Rivers in Southwest France. *Sci. Total Environ.* **2002**, *298*, 103–118. [CrossRef] [PubMed]
51. Pohlert, T.; Hillebrand, G.; Breitung, V. Effects of Sampling Techniques on Physical Parameters and Concentrations of Selected Persistent Organic Pollutants in Suspended Matter. *J. Environ. Monit.* **2011**, *13*, 1579–1588. [CrossRef] [PubMed]
52. Liu, H.; Li, Q.; Shi, T.; Hu, S.; Wu, G.; Zhou, Q. Application of Sentinel 2 MSI Images to Retrieve Suspended Particulate Matter Concentrations in Poyang Lake. *Remote Sens.* **2017**, *9*, 761. [CrossRef]
53. Wen, Z.; Wang, Q.; Ma, Y.; Jacinthe, P.A.; Liu, G.; Li, S.; Shang, Y.; Tao, H.; Fang, C.; Lyu, L.; et al. Remote Estimates of Suspended Particulate Matter in Global Lakes Using Machine Learning Models. *Int. Soil Water Conserv. Res.* **2024**, *12*, 200–216. [CrossRef]
54. Schubert, B.; Heininger, P.; Keller, M.; Claus, E.; Ricking, M. Monitoring of Contaminants in Suspended Particulate Matter as an Alternative to Sediments. *TrAC Trends Anal. Chem.* **2012**, *36*, 58–70. [CrossRef]
55. Rossé, P.; Vignati, D.; Dominik, J. Effects of Continuous Flow Centrifugation on Measurements of Trace Elements in River Water: Intrinsic Contamination and Particle Fragmentation. *Hydrol. Process.* **2006**, *20*, 2745–2754. [CrossRef]
56. Buffle, J.; Perret, D.; Newman, M. The Use of Filtration and Ultrafiltration for Size Fractionation of Aquatic Particles, Colloids, and Macromolecules. In *Environmental Particles*; CRC Press: Boca Raton, FL, USA, 2019; pp. 171–230.
57. Masson, M.; Angot, H.; Le Bescond, C.; Launay, M.; Dabrin, A.; Miege, C.; Le Coz, J.; Coquery, M. Sampling of Suspended Particulate Matter Using Particle Traps in the Rhône River: Relevance and Representativeness for the Monitoring of Contaminants. *Sci. Total Environ.* **2018**, *637*, 538–549. [CrossRef] [PubMed]
58. Moody, J.A.; Meade, R.H. Evaluation of the Method of Collecting Suspended Sediment from Large Rivers by Discharge-weighted Pumping and Separation by Continuous-flow Centrifugation. *Hydrol. Process.* **1994**, *8*, 513–530. [CrossRef]
59. Breitung, V. Probenahme Mit Einer Durchlaufzentrifuge Zur Gewinnung von Schwebstoffen Für Die Schadstoffanalyse Aus Fließenden Gewässern. *Dtsch. Gewässerkundliche Mitteilungen* **1997**, *41*, 113–117.
60. Burrus, D.; Thomas, R.L.; Dominik, J.; Vernet, J. Recovery and Concentration of Suspended Solids in the Upper Rhone River by Continuous Flow Centrifugation. *Hydrol. Process.* **1989**, *3*, 65–74. [CrossRef]
61. Keßler, S.; Pohlert, T.; Breitung, V.; Wilcsek, K.; Bierl, R. Comparative Evaluation of Four Suspended Particulate Matter (SPM) Sampling Devices and Their Use for Monitoring SPM Quality. *Environ. Sci. Pollut. Res.* **2020**, *27*, 5993–6008. [CrossRef] [PubMed]
62. Baborowski, M.; Claus, E.; Friese, K.; Von der Kammer, F.; Kasimir, P.; Pelzer, J.; Heininger, P. Comparison of Different Monitoring Programs of the 2002 Summer Flood in the River Elbe. *Acta Hydrochim. Hydrobiol.* **2005**, *33*, 404–417. [CrossRef]
63. Abuhelou, F.; Mansuy-Huault, L.; Lorgeoux, C.; Catteloin, D.; Collin, V.; Bauer, A.; Kanbar, H.J.; Gley, R.; Manceau, L.; Thomas, F.; et al. Suspended Particulate Matter Collection Methods Influence the Quantification of Polycyclic Aromatic Compounds in the River System. *Environ. Sci. Pollut. Res.* **2017**, *24*, 22717–22729. [CrossRef] [PubMed]
64. Hildebrandt, L.; Zimmermann, T.; Primpke, S.; Fischer, D.; Gerdts, G.; Pröfrock, D. Comparison and Uncertainty Evaluation of Two Centrifugal Separators for Microplastic Sampling. *J. Hazard. Mater.* **2021**, *414*, 125482. [CrossRef] [PubMed]
65. Schulze, T.; Ricking, M.; Schröter-Kermani, C.; Körner, A.; Denner, H.-D.; Weinfurtner, K.; Winkler, A.; Pekdeger, A. The German Environmental Specimen Bank: Sampling, Processing, and Archiving Sediment and Suspended Particulate Matter. *J. Soils Sediments* **2007**, *7*, 361–367.
66. Horowitz, A.J.; Elrick, K.A.; Hooper, R.C. A Comparison of Instrumental Dewatering Methods for the Separation and Concentration of Suspended Sediment for Subsequent Trace Element Analysis. *Hydrol. Process.* **1989**, *3*, 163–184. [CrossRef]
67. Rees, T.F.; Leenheer, J.A.; Ranville, J.F. Use of a Single-bowl Continuous-flow Centrifuge for Dewatering Suspended Sediments: Effect on Sediment Physical and Chemical Characteristics. *Hydrol. Process.* **1991**, *5*, 201–214. [CrossRef]
68. Liu, Y.; Cheng, Q.; Zhang, B.; Tian, F. Three-Phase Hydrocyclone Separator—A Review. *Chem. Eng. Res. Des.* **2015**, *100*, 554–560. [CrossRef]
69. Pohlert, T. *Vergleich Neuartiger Geräte Zur Schwebstoffgewinnung Für Das Chemische Gewässermonitoring—SCHWEBSAM: Ein Forschungs—Und Entwicklungsprojekt Der Bundesanstalt Für Gewässerkunde und Der Universität Trier*; Bundesanstalt für Gewässerkunde: Koblenz, Germany, 2015.
70. Gaumert, T. *Entwicklung Der Schadstoffgehalte in Frischen, Schwebstoffbürtigen Sedimenten Der Elbe Bei Schnackenburg: 1984–1991*; Arge Elbe: Magdeburg, Germany, 1992.
71. Phillips, J.M.; Russell, M.A.; Walling, D.E. Time-integrated Sampling of Fluvial Suspended Sediment: A Simple Methodology for Small Catchments. *Hydrol. Process.* **2000**, *14*, 2589–2602. [CrossRef]
72. Laceby, J.P.; Evrard, O.; Smith, H.G.; Blake, W.H.; Olley, J.M.; Minella, J.P.G.; Owens, P.N. The Challenges and Opportunities of Addressing Particle Size Effects in Sediment Source Fingerprinting: A Review. *Earth-Sci. Rev.* **2017**, *169*, 85–103. [CrossRef]
73. Giddings, J.C. Field-Flow Fractionation: Analysis of Macromolecular, Colloidal, and Particulate Materials. *Science* **1993**, *260*, 1456–1465. [CrossRef] [PubMed]

74. Ulrich, A.; Losert, S.; Bendixen, N.; Al-Kattan, A.; Hagendorfer, H.; Nowack, B.; Adlhart, C.; Ebert, J.; Lattuada, M.; Hungerbühler, K. Critical Aspects of Sample Handling for Direct Nanoparticle Analysis and Analytical Challenges Using Asymmetric Field Flow Fractionation in a Multi-Detector Approach. *J. Anal. At. Spectrom.* **2012**, *27*, 1120–1130. [CrossRef]
75. Hassellöv, M.; von der Kammer, F.; Beckett, R. Characterisation of Aquatic Colloids and Macromolecules by Field-Flow Fractionation. *Environ. Colloids Part. Behav. Sep. Characterisation* **2006**, *10*, 223–276. [CrossRef]
76. Floge, S.A.; Wells, M.L. Variation in Colloidal Chromophoric Dissolved Organic Matter in the Damariscotta Estuary, Maine. *Limnol. Oceanogr.* **2007**, *52*, 32–45. [CrossRef]
77. Stolpe, B.; Guo, L.; Shiller, A.M.; Hassellöv, M. Size and Composition of Colloidal Organic Matter and Trace Elements in the Mississippi River, Pearl River and the Northern Gulf of Mexico, as Characterized by Flow Field-Flow Fractionation. *Mar. Chem.* **2010**, *118*, 119–128. [CrossRef]
78. Chittleborough, D.J.; Tadjiki, S.; Ranville, J.F.; Shanks, F.; Beckett, R. Soil Colloid Analysis by Flow Field-Flow Fractionation. In Proceedings of the 3rd Australian New Zealand Soils Conference, Symposium, Sydney, Australia, 5–9 December 2004; Volume 4.
79. Harhash, M.; Schroeder, H.; Zavarsky, A.; Kamp, J.; Linkhorst, A.; Lauschke, T.; Dierkes, G.; Ternes, T.A.; Duester, L. Efficiency of Five Samplers to Trap Suspended Particulate Matter and Microplastic Particles of Different Sizes. *Chemosphere* **2023**, *338*, 139479. [CrossRef] [PubMed]
80. Matos, T.; Martins, M.S.; Henriques, R.; Gonçalves, L.M. Design of a Sensor to Estimate Suspended Sediment Transport In Situ Using the Measurements of Water Velocity, Suspended Sediment Concentration and Depth. *J. Environ. Manag.* **2024**, *365*, 121660. [CrossRef] [PubMed]
81. Droujko, J.; Molnar, P. Open-Source, Low-Cost, In-Situ Turbidity Sensor for River Network Monitoring. *Sci. Rep.* **2022**, *12*, 10501. [CrossRef] [PubMed]
82. Kim, J.; Kwon, S.; Chung, S.; Kim, Y. Do Turbidity and Suspended Sediment Relationship Based on Sediment Composition and Particle Size Distribution. *Sci. Rep.* **2025**, *15*, 16286. [CrossRef] [PubMed]
83. Nord, G.; Michielin, Y.; Biron, R.; Esteves, M.; Freche, G.; Geay, T.; Hauet, A.; Legoût, C.; Mercier, B. An Autonomous Low-Power Instrument Platform for Monitoring Water and Solid Discharges in Mesoscale Rivers. *Geosci. Instrum. Methods Data Syst.* **2020**, *9*, 41–67. [CrossRef]
84. Macht, F.; Eusterhues, K.; Pronk, G.J.; Totsche, K.U. Specific Surface Area of Clay Minerals: Comparison between Atomic Force Microscopy Measurements and Bulk-Gas (N2) and-Liquid (EGME) Adsorption Methods. *Appl. Clay Sci.* **2011**, *53*, 20–26. [CrossRef]
85. Brunauer, S.; Emmett, P.H.; Teller, E. Adsorption of Gases in Multimolecular Layers. *J. Am. Chem. Soc.* **1938**, *60*, 309–319. [CrossRef]
86. De Boer, J.H.; Lippens, B.C.; Linsen, B.G.; Broekhoff, J.C.P.; Van den Heuvel, A.; Osinga, T.J. Thet-Curve of Multimolecular N2-Adsorption. *J. Colloid Interface Sci.* **1966**, *21*, 405–414. [CrossRef]
87. Barrett, E.P.; Joyner, L.G.; Halenda, P.P. The Determination of Pore Volume and Area Distributions in Porous Substances. I. Computations from Nitrogen Isotherms. *J. Am. Chem. Soc.* **1951**, *73*, 373–380. [CrossRef]
88. Clausen, L.; Fabricius, I. BET Measurements: Outgassing of Minerals. *J. Colloid Interface Sci.* **2000**, *227*, 7–15. [CrossRef] [PubMed]
89. Thomas, J.; Bohor, B.F. Surface Area of Montmorillonite from the Dynamic Sorption of Nitrogen and Carbon Dioxide. *Clays Clay Miner.* **1968**, *16*, 83–91. [CrossRef]
90. Hofmann, A.; Vantelon, D.; Montarges-Pelletier, E.; Villain, F.; Gardoll, O.; Razafitianamaharavo, A.; Ghanbaja, J. Interaction of Fe(III) and Al(III) during Hydroxylation by Forced Hydrolysis: The Nature of Al-Fe Oxyhydroxy Co-Precipitates. *J. Colloid Interface Sci.* **2013**, *407*, 76–88. [CrossRef] [PubMed]
91. Carter, D.L.; Heilman, M.D.; Gonzales, C.L. Ethylene Glycol Monoethyl Ether for Determining Surface Area of Silicate Minerals. *Soil Sci.* **1965**, *100*, 356–360. [CrossRef]
92. Johnston, C.T.; Tombácz, E. Surface Chemistry of Soil Minerals. *Soil Mineral. Environ. Appl.* **2002**, *7*, 37–67. [CrossRef]
93. Kaufhold, S.; Dohrmann, R.; Klinkenberg, M.; Siegesmund, S.; Ufer, K. N2-BET Specific Surface Area of Bentonites. *J. Colloid Interface Sci.* **2010**, *349*, 275–282. [CrossRef] [PubMed]
94. Michot, L.J.; Villiéras, F. Chapter 12.9 Surface Area and Porosity. In *Handbook of Clay Science*; Bergaya, F., Theng, B.K.G., Lagaly, G., Eds.; Elsevier: Amsterdam, The Netherlands, 2006; Volume 1, pp. 965–978.
95. Bibby, R.L.; Webster-Brown, J.G. Characterisation of Urban Catchment Suspended Particulate Matter (Auckland Region, New Zealand); a Comparison with Non-Urban SPM. *Sci. Total Environ.* **2005**, *343*, 177–197. [CrossRef] [PubMed]
96. Dzombak, D.A.; Morel, F.M. *Surface Complexation Modeling: Hydrous Ferric Oxide*; John Wiley & Sons: New York, NY, USA, 1990.
97. Horowitz, A.J.; Elrick, K.A. The Relation of Stream Sediment Surface Area, Grain Size and Composition to Trace Element Chemistry. *Appl. Geochem.* **1987**, *2*, 437–451. [CrossRef]
98. Jilbert, T.; Asmala, E.; Schröder, C.; Tiihonen, R.; Myllykangas, J.-P.; Virtasalo, J.J.; Kotilainen, A.; Peltola, P.; Ekholm, P.; Hietanen, S. Impacts of Flocculation on the Distribution and Diagenesis of Iron in Boreal Estuarine Sediments. *Biogeosciences* **2018**, *15*, 1243–1271. [CrossRef]

99. Chen, L.C.; Lippmann, M. Effects of Metals Within Ambient Air Particulate Matter (PM) on Human Health. *Inhal. Toxicol.* **2009**, *21*, 1–31. [CrossRef] [PubMed]
100. Panwichian, S.; Kantachote, D.; Wittayaweerasak, B.; Mallavarapu, M. Removal of Heavy Metals by Exopolymeric Substances Produced by Resistant Purple Nonsulfur Bacteria Isolated from Contaminated Shrimp Ponds. *Electron. J. Biotechnol.* **2011**, *14*, 2. [CrossRef]
101. Douvris, C.; Bentil, E.; Ayensu, I.; Osei Akoto, C.; Amponsah, I.K.; Adu, J.; Bussan, D. Trace Metals in Cannabis Seized by Law Enforcement in Ghana and Multivariate Analysis to Distinguish among Different Cannabis Farms. *Toxics* **2022**, *10*, 567. [CrossRef] [PubMed]
102. Mitra, S. *Sample Preparation Techniques in Analytical Chemistry*; John Wiley & Sons: Hoboken, NJ, USA, 2003.
103. Kurfürst, U. *Solid Sample Analysis Direct and Slurry Sampling Using GF-AAS and ETV-ICP*; Springer: London, UK, 2011.
104. Carignan, J.; Hild, P.; Mevelle, G.; Morel, J.; Yeghicheyan, D. Routine Analyses of Trace Elements in Geological Samples Using Flow Injection and Low Pressure On-Line Liquid Chromatography Coupled to ICP-MS: A Study of Geochemical Reference Materials BR, DR-N, UB-N, AN-G and GH. *Geostand. Geoanalytical Res.* **2001**, *25*, 187–198. [CrossRef]
105. Zhang, W.; Hu, Z.; Liu, Y. Recent Advances in Sample Preparation Methods for Elemental and Isotopic Analysis of Geological Samples. *Spectrochim. Acta Part B At. Spectrosc.* **2019**, *160*, 105690. [CrossRef]
106. Walkner, C.; Gratzer, R.; Meisel, T.; Bokhari, S.N.H. Multi-Element Analysis of Crude Oils Using ICP-QQQ-MS. *Org. Geochem.* **2017**, *103*, 22–30. [CrossRef]
107. Garzanti, E.; Andó, S.; France-Lanord, C.; Censi, P.; Vignola, P.; Galy, V.; Lupker, M. Mineralogical and Chemical Variability of Fluvial Sediments 2. Suspended-Load Silt (Ganga–Brahmaputra, Bangladesh). *Earth Planet. Sci. Lett.* **2011**, *302*, 107–120. [CrossRef]
108. Martin, J.M.; Meybeck, M. Elemental Mass-Balance of Material Carried by Major World Rivers. *Mar. Chem.* **1979**, *7*, 173–206. [CrossRef]
109. Xia, Z.; Zhang, J.; Yan, Y.; Zhang, W.; Zhao, Z. Heavy Metals in Suspended Particulate Matter in the Yarlung Tsangpo River, Southwest China. *Geosyst. Geoenviron.* **2024**, *3*, 100160. [CrossRef]
110. Chen, J.; Liu, M.; Wang, F.; Ding, Y.; Fan, D.; Wang, H. Accumulation and Migration of Particulate Trace Metals by Artificial Flood Event of the Yellow River: From Xiaolangdi Reservoir to Estuary. *Sci. Total Environ.* **2024**, *912*, 168614. [CrossRef] [PubMed]
111. Wang, P.; Hu, J.; Liu, T.; Liu, J.; Ma, S.; Ma, W.; Li, J.; Zheng, H.; Lu, R. Advances in the Application of Metallic Isotopes to the Identification of Contaminant Sources in Environmental Geochemistry. *J. Hazard. Mater.* **2023**, *458*, 131913. [CrossRef] [PubMed]
112. Baskaran, M. *Handbook of Environmental Isotope Geochemistry*; Springer Science & Business Media: Berlin/Heidelberg, Germany, 2011.
113. Barnes, I.L.; Murphy, T.J.; Gramlich, J.W.; Shields, W.R. Lead Separation by Anodic Deposition and Isotope Ratio Mass Spectrometry of Microgram and Smaller Samples. *Anal. Chem.* **1973**, *45*, 1881–1884. [CrossRef]
114. Wang, L.; Jin, Y.; Weiss, D.J.; Schleicher, N.J.; Wilcke, W.; Wu, L.; Guo, Q.; Chen, J.; O'Connor, D.; Hou, D. Possible Application of Stable Isotope Compositions for the Identification of Metal Sources in Soil. *J. Hazard. Mater.* **2021**, *407*, 124812. [CrossRef] [PubMed]
115. Desaulty, A.-M.; Petelet-Giraud, E. Zinc Isotope Composition as a Tool for Tracing Sources and Fate of Metal Contaminants in Rivers. *Sci. Total Environ.* **2020**, *728*, 138599. [CrossRef] [PubMed]
116. Li, Y.; Huang, Y.; Li, Z.; Tang, X.; Liu, X.; Hughes, S.S. Mechanisms of Chromium Isotope Fractionation and the Applications in the Environment. *Ecotoxicol. Environ. Saf.* **2022**, *242*, 113948. [CrossRef] [PubMed]
117. Zhang, R.; Meija, J.; Huang, Y.; Pei, X.; Mester, Z.; Yang, L. Determination of the Isotopic Composition of Tungsten Using MC-ICP-MS. *Anal. Chim. Acta* **2019**, *1089*, 19–24. [CrossRef] [PubMed]
118. Stürup, S.; Hansen, H.R.; Gammelgaard, B. Application of Enriched Stable Isotopes as Tracers in Biological Systems: A Critical Review. *Anal. Bioanal. Chem.* **2008**, *390*, 541–554. [CrossRef] [PubMed]
119. Croteau, M.-N.; Cain, D.J.; Fuller, C.C. Novel and Nontraditional Use of Stable Isotope Tracers to Study Metal Bioavailability from Natural Particles. *Environ. Sci. Technol.* **2013**, *47*, 3424–3431. [CrossRef] [PubMed]
120. von Blanckenburg, F.; Willenbring, J.K. Cosmogenic Nuclides: Dates and Rates of Earth-Surface Change. *Elements* **2014**, *10*, 341–346. [CrossRef]
121. Lee, C.; Kim, N.B.; Lee, I.C.; Chung, K.S. The Use of a Chelating Resin Column for Preconcentration of Trace Elements from Sea-Water in Their Determination by Neutron-Activation Analysis. *Talanta* **1977**, *24*, 241–245. [CrossRef] [PubMed]
122. Żmijewska, W.; Polkowska-Motrenko, H.; Stokowska, H. Preconcentration of Trace Elements from Water by Coprecipitation and Ion Exchange. *J. Radioanal. Nucl. Chem.* **1984**, *84*, 319–328. [CrossRef]
123. Vance, D.; Matthews, A.; Keech, A.; Archer, C.; Hudson, G.; Pett-Ridge, J.; Chadwick, O.A. The Behaviour of Cu and Zn Isotopes during Soil Development: Controls on the Dissolved Load of Rivers. *Chem. Geol.* **2016**, *445*, 36–53. [CrossRef]
124. Xia, Y.; Gao, T.; Liu, Y.; Wang, Z.; Liu, C.; Wu, Q.; Qi, M.; Lv, Y.; Li, F. Zinc Isotope Revealing Zinc's Sources and Transport Processes in Karst Region. *Sci. Total Environ.* **2020**, *724*, 138191. [CrossRef] [PubMed]

125. Ding, Z.; Han, G.; Qu, R.; Liu, J.; Wang, P. Review on Zinc Isotopes in River Systems: Distribution and Application. *Water* **2024**, *16*, 87. [CrossRef]
126. Petit, J.C.J.; De Jong, J.; Chou, L.; Mattielli, N. Development of Cu and Zn Isotope MC-ICP-MS Measurements: Application to Suspended Particulate Matter and Sediments from the Scheldt Estuary. *Geostand. Geoanal. Res.* **2008**, *32*, 149–166. [CrossRef]
127. Zimmermann, T.; Mohamed, A.F.; Reese, A.; Wieser, M.E.; Kleeberg, U.; Pröfrock, D.; Irrgeher, J. Zinc Isotopic Variation of Water and Surface Sediments from the German Elbe River. *Sci. Total Environ.* **2020**, *707*, 135219. [CrossRef] [PubMed]
128. Kimball, B.E. Biogeochemical Cycling of Copper in Acid Mine Drainage. Ph.D. Thesis, The Pennsylvania State University, University Park, PA, USA, 2009.
129. Zeng, J.; Han, G. Preliminary Copper Isotope Study on Particulate Matter in Zhujiang River, Southwest China: Application for Source Identification. *Ecotoxicol. Environ. Saf.* **2020**, *198*, 110663. [CrossRef] [PubMed]
130. Cristina Vásquez, A.; Razak, N.S.A.; Hohl, S.; He, Z. Dissolved Trace Metal Sources and Copper Isotopic Fractionation in a Tropical Volcanic River–Insights for Small Mountainous River Systems. *J. Geochem. Explor.* **2026**, *287*, 108077. [CrossRef]
131. Song, S.; Mathur, R.; Ruiz, J.; Chen, D.; Allin, N.; Guo, K.; Kang, W. Fingerprinting Two Metal Contaminants in Streams with Cu Isotopes near the Dexing Mine, China. *Sci. Total Environ.* **2016**, *544*, 677–685. [CrossRef] [PubMed]
132. Brown, G.; Brindley, G.W. X-Ray Diffraction Procedures for Clay Mineral Identification. In *Crystal Structures of Clay Minerals and Their X-Ray Identification*; Brindley, G.W., Brown, G., Eds.; Mineralogical Society: London, UK, 1980; pp. 305–359.
133. Rancourt, D.G.; Dang, M.Z. Absolute Quantification by Powder X-Ray Diffraction of Complex Mixtures of Crystalline and Amorphous Phases for Applications in the Earth Sciences. *Am. Mineral.* **2005**, *90*, 1571–1586. [CrossRef]
134. Poppe, L.J.; Paskevich, V.F.; Hathaway, J.C.; Blackwood, D.S. *A Laboratory Manual for X-Ray Powder Diffraction*; US Geological Survey: Reston, VA, USA, 2001.
135. Holder, C.F.; Schaak, R.E. Tutorial on Powder X-Ray Diffraction for Characterizing Nanoscale Materials. *ACS Nano* **2019**, *13*, 7359–7365. [CrossRef] [PubMed]
136. Bortoluzzi, E.C.; dos Santos, D.R.; Santanna, M.A.; Caner, L. Mineralogy and Nutrient Desorption of Suspended Sediments during a Storm Event. *J. Soils Sediments* **2013**, *13*, 1093–1105. [CrossRef]
137. River, M.; Richardson, C.J. Suspended Sediment Mineralogy and the Nature of Suspended Sediment Particles in Stormflow of the Southern Piedmont of the USA. *Water Resour. Res.* **2019**, *55*, 5665–5678. [CrossRef]
138. Mackowiak, T.J.; Perdrial, N. Monitoring of Suspended Sediment Mineralogy in Puerto-Rican Rivers: Effects of Flowrate and Lithology. *Minerals* **2023**, *13*, 208. [CrossRef]
139. Legout, C.; Poulenard, J.; Nemery, J.; Navratil, O.; Grangeon, T.; Evrard, O.; Esteves, M. Quantifying Suspended Sediment Sources during Runoff Events in Headwater Catchments Using Spectrocolorimetry. *J. Soils Sediments* **2013**, *13*, 1478–1492. [CrossRef]
140. Martínez-Carreras, N.; Krein, A.; Udelhoven, T.; Gallart, F.; Iffly, J.F.; Hoffmann, L.; Pfister, L.; Walling, D.E. A Rapid Spectral-Reflectance-Based Fingerprinting Approach for Documenting Suspended Sediment Sources during Storm Runoff Events. *J. Soils Sediments* **2010**, *10*, 400–413. [CrossRef]
141. Brosinsky, A.; Foerster, S.; Segl, K.; López-Tarazón, J.A.; Piqué, G.; Bronstert, A. Spectral Fingerprinting: Characterizing Suspended Sediment Sources by the Use of VNIR-SWIR Spectral Information. *J. Soils Sediments* **2014**, *14*, 1965–1981. [CrossRef]
142. Poulenard, J.; Perrette, Y.; Fanget, B.; Quetin, P.; Trevisan, D.; Dorioz, J.M. Infrared Spectroscopy Tracing of Sediment Sources in a Small Rural Watershed (French Alps). *Sci. Total Environ.* **2009**, *407*, 2808–2819. [CrossRef] [PubMed]
143. Tiecher, T.; Caner, L.; Minella, J.P.G.; Bender, M.A.; dos Santos, D.R. Tracing Sediment Sources in a Subtropical Rural Catchment of Southern Brazil by Using Geochemical Tracers and Near-Infrared Spectroscopy. *Soil Tillage Res.* **2016**, *155*, 478–491. [CrossRef]
144. Madejová, J.; Gates, W.P.; Petit, S. IR Spectra of Clay Minerals. In *Developments in Clay Science*; Gates, W.P., Kloprogge, J.T., Madejová, J., Bergaya, F., Eds.; Eslevier: Amsterdam, The Netherlands, 2017; Volume 8, pp. 107–149.
145. Parikh, S.J.; Goyne, K.W.; Margenot, A.J.; Calderón, F.J. Soil Chemical Insights Provided through Vibrational Spectroscopy. In *Advances in Agronomy*; Eslevier: Amsterdam, The Netherlands, 2014; Volume 126, pp. 1–148.
146. De Lorenzi Pezzolo, A. An Exercise on Calibration: DRIFTS Study of Binary Mixtures of Calcite and Dolomite with Partially Overlapping Spectral Features. *J. Chem. Educ.* **2013**, *90*, 118–122. [CrossRef]
147. Vogel, H.; Rosén, P.; Wagner, B.; Melles, M.; Persson, P. Fourier Transform Infrared Spectroscopy, a New Cost-Effective Tool for Quantitative Analysis of Biogeochemical Properties in Long Sediment Records. *J. Paleolimnol.* **2008**, *40*, 689–702. [CrossRef]
148. Hahn, A.; Vogel, H.; Andó, S.; Garzanti, E.; Kuhn, G.; Lantzsch, H.; Schüürman, J.; Vogt, C.; Zabel, M. Using Fourier Transform Infrared Spectroscopy to Determine Mineral Phases in Sediments. *Sediment. Geol.* **2018**, *375*, 27–35. [CrossRef]
149. Felten, J.; Hall, H.; Jaumot, J.; Tauler, R.; De Juan, A.; Gorzsás, A. Vibrational Spectroscopic Image Analysis of Biological Material Using Multivariate Curve Resolution-Alternating Least Squares (MCR-ALS). *Nat. Protoc.* **2015**, *10*, 217–240. [CrossRef] [PubMed]
150. Felten, J.; Hall, H.; Jaumot, J.; Tauler, R.; de Juan, A.; Gorzsás, A. Addendum: Vibrational Spectroscopic Image Analysis of Biological Material Using Multivariate Curve Resolution–Alternating Least Squares (MCR-ALS). *Nat. Protoc.* **2019**, *14*, 3032. [CrossRef] [PubMed]

151. Mas, S.; Bendoula, R.; Agoda-Tandjawa, G.; de Juan, A.; Roger, J.-M. Study of Time-Dependent Structural Changes of Laponite Colloidal System by Means of near-Infrared Spectroscopy and Hybrid Hard- and Soft-Modelling Multivariate Curve Resolution–Alternating Least Squares. *Chemom. Intell. Lab. Syst.* **2015**, *142*, 285–292. [CrossRef]
152. Kanbar, H.J.; Tran Le, T.; Olajos, F.; Englund, G.; Holmboe, M. Tracking Mineral and Geochemical Characteristics of Holocene Lake Sediments: The Case of Hotagen, West-Central Sweden. *J. Soils Sediments* **2021**, *21*, 3150–3168. [CrossRef]
153. Kanbar, H.J.; Olajos, F.; Englund, G.; Holmboe, M. Geochemical Identification of Potential DNA-Hotspots and DNA-Infrared Fingerprints in Lake Sediments. *Appl. Geochem.* **2020**, *122*, 104728. [CrossRef]
154. Verheyen, D.; Diels, J.; Kissi, E.; Poesen, J. The Use of Visible and Near-Infrared Reflectance Measurements for Identifying the Source of Suspended Sediment in Rivers and Comparison with Geochemical Fingerprinting. *J. Soils Sediments* **2014**, *14*, 1869–1885. [CrossRef]
155. Lartiges, B.S.; Deneux-Mustin, S.; Villemin, G.; Mustin, C.; Barrès, O.; Chamerois, M.; Gerard, B.; Babut, M. Composition, Structure and Size Distribution of Suspended Particulates from the Rhine River. *Water Res.* **2001**, *35*, 808–816. [CrossRef] [PubMed]
156. Gredilla, A.; Fdez-Ortiz de Vallejuelo, S.; Gomez-Nubla, L.; Aramendia, J.; Ruiz-Romera, E.; de Diego, A.; Antigüedad, I.; Madariaga, J.M. Raman Spectroscopy to Investigate the Speciation and Origin of Hazardous Elements Associated to Suspended Particulate Matter during a Large Flood Event. *J. Raman Spectrosc.* **2020**, *51*, 1480–1492. [CrossRef]
157. Kaskes, P.; Déhais, T.; de Graaff, S.J.; Goderis, S.; Claeys, P. Micro–X-Ray Fluorescence (MXRF) Analysis of Proximal Impactites: High-Resolution Element Mapping, Digital Image Analysis, and Quantifications. *Spec. Pap. Geol. Soc. Am.* **2021**, *550*, 171–206. [CrossRef]
158. Almeida, A.P.F.; Leitão, R.; de Araujo, Á.R.; Teles, Á.d.P.; Barbosa, A.d.S.; Assis, J.; Anjos, M.; Lopes, R.; Olivera, D. Determination of Trace Elements in Particulate Matter From an Urban Area Near an Industrial Complex by Micro-XRF. *X-Ray Spectrom.* **2026**, *55*, 407–420. [CrossRef]
159. Soromotin, A.; Moskovchenko, D.; Khoroshavin, V.; Prikhodko, N.; Puzanov, A.; Kirillov, V.; Koveshnikov, M.; Krylova, E.; Krasnenko, A.; Pechkin, A. Major, Trace and Rare Earth Element Distribution in Water, Suspended Particulate Matter and Stream Sediments of the Ob River Mouth. *Water* **2022**, *14*, 2442. [CrossRef]
160. Osán, J.; Török, S.; Alföldy, B.; Alsecz, A.; Falkenberg, G.; Baik, S.Y.; Van Grieken, R. Comparison of Sediment Pollution in the Rivers of the Hungarian Upper Tisza Region Using Non-Destructive Analytical Techniques. *Spectrochim. Acta-Part B At. Spectrosc.* **2007**, *62*, 123–136. [CrossRef]
161. Schindelin, J.; Arganda-Carreras, I.; Frise, E.; Kaynig, V.; Longair, M.; Pietzsch, T.; Preibisch, S.; Rueden, C.; Saalfeld, S.; Schmid, B.; et al. Fiji: An Open-Source Platform for Biological-Image Analysis. *Nat. Methods* **2012**, *9*, 676–682. [CrossRef]
162. Jantzi, S.C.; Dutton, C.L.; Saha, A.; Masikini, R.; Almirall, J.R. Novel "Filter Pellet" Sample Preparation Strategy for Quantitative LA-ICP-MS Analysis of Filter-Bound Sediments: A "Green Chemistry" Alternative to Sediment Fingerprinting in Tanzania's Ruvu River Basin. *J. Soils Sediments* **2019**, *19*, 478–490. [CrossRef]
163. Paton, L.; Kiesel, S.; Steinhoefel, G.; Elinkmann, M.; Moro, T.T.; Gonzalez de Vega, R.; Bohleber, P.; Clases, D. Assessing the Impact of Common Sample Preparation Strategies for Single Particle ICP-MS Regarding Recovery and Size Distribution of Natural Single Particles. *J. Anal. At. Spectrom.* **2025**, *40*, 2897–2908. [CrossRef] [PubMed]
164. Ji, H.; Ding, H.; Tang, L.; Li, C.; Gao, Y.; Briki, M. Chemical Composition and Transportation Characteristic of Trace Metals in Suspended Particulate Matter Collected Upstream of a Metropolitan Drinking Water Source, Beijing. *J. Geochem. Explor.* **2016**, *169*, 123–136. [CrossRef]
165. Liu, W.; Lu, G.; Wang, W.-X. In Situ High-Resolution Two-Dimensional Profiles of Redox Sensitive Metal Mobility in Sediment-Water Interface and Porewater from Estuarine Sediments. *Sci. Total Environ.* **2022**, *820*, 153034. [CrossRef] [PubMed]
166. Menegatti, C.R.; Cavalcante, M.S.; Schneider, R.; Pontes, G.; Senesi, G.S.; Nicolodelli, G. Direct Laser-Induced Breakdown Spectroscopy Analysis of Estuarine Suspended Particulate Matter Collected on Filters. *Molecules* **2026**, *31*, 647. [CrossRef] [PubMed]
167. Pinet, S.; Lartiges, B.; Martinez, J.-M.; Ouillon, S. A SEM-Based Method to Determine the Mineralogical Composition and the Particle Size Distribution of Suspended Sediment. *Int. J. Sediment Res.* **2019**, *34*, 85–94. [CrossRef]
168. de Boer, D.H.; Crosby, G. Evaluating the Potential of SEM/EDS Analysis for Fingerprinting Suspended Sediment Derived from Two Contrasting Topsoils. *Catena* **1995**, *24*, 243–258. [CrossRef]
169. Haley, S.M.; Tappin, A.D.; Bond, P.R.; Fitzsimons, M.F. A Comparison of SEM-EDS with ICP-AES for the Quantitative Elemental Determination of Estuarine Particles. *Environ. Chem. Lett.* **2006**, *4*, 235–238. [CrossRef]
170. Jin, X.; Zhang, W.; Zhu, Y.; Shan, B. Characteristics of Suspended Particulate Matter in a Typical Slow-Moving River of Northern China: Insight into Its Structure and Motion Behavior. *Chemosphere* **2018**, *202*, 521–529. [CrossRef] [PubMed]
171. Liu, X.; Wang, Y.; Zhang, Q.; Liu, C.; Song, Y.; Li, Y.; Yin, Y.; Cai, Y. Confounding Effects of Seasonality and Anthropogenic River Regulation on Suspended Particulate Matter-Driven Mercury Transport to Coastal Seas. *J. Hazard. Mater.* **2024**, *469*, 133979. [CrossRef] [PubMed]

172. Taylor, R.J.M.; Hill, E.; Andrew, M. A Step Forward in Quantitative Automated Mineralogy in 2D and 3D. *Geostand. Geoanal. Res.* **2024**, *48*, 579–593. [CrossRef]
173. Laureano, F.V.; Kwitko-Ribeiro, R.; Guimarães, L.; Leão, L.P. Mineralogical Fingerprint of Iron Ore Tailings in Paraopeba River Bedload Sediments after the B1 Dam Failure in Brumadinho, MG (Brazil). *Minerals* **2022**, *12*, 716. [CrossRef]
174. Sindern, S.; Tremöhlen, M.; Dsikowitzky, L.; Gronen, L.; Schwarzbauer, J.; Siregar, T.H.; Ariyani, F.; Irianto, H.E. Heavy Metals in River and Coast Sediments of the Jakarta Bay Region (Indonesia)—Geogenic versus Anthropogenic Sources. *Mar. Pollut. Bull.* **2016**, *110*, 624–633. [CrossRef] [PubMed]
175. Gottlieb, P.; Wilkie, G.; Sutherland, D.; Ho-Tun, E. Using Quantitative Electron Microscopy for Process Mineralogy Applications. *JOM* **2000**, *52*, 24. [CrossRef]
176. Saberi, N.; Vriens, B. Sample Preparation Biases in Automated Quantitative Mineralogical Analysis of Mine Wastes. *Microsc. Microanal.* **2023**, *29*, 94–104. [CrossRef]
177. Johnson, D.; Rollinson, G.K.; Arif, A.T.; Moreno, T.; Ruiz, P.T.; Lah, R.; Lubosik, Z.; Pindel, T.; Gminsk, R.; Williamson, B.J. QEMSCAN® Automated Mineralogical Analysis of PM2. 5 and PM4: A Preliminary Study of Underground Coal Mine Dust from Poland and Slovenia. *Front. Earth Sci.* **2022**, *10*, 788928. [CrossRef]
178. Schulz, B. Editorial for Special Issue "Applications of SEM Automated Mineralogy: From Ore Deposits over Processing to Secondary Resource Characterization". *Minerals* **2020**, *10*, 1103. [CrossRef]
179. Pirrie, D.; Butcher, A.R.; Power, M.R.; Gottlieb, P.; Miller, G.L. *Rapid Quantitative Mineral and Phase Analysis Using Automated Scanning Electron Microscopy (QemSCAN)*; Potential Applications in Forensic Geoscience; Geological Society of London: London, UK, 2004.
180. Fandrich, R.; Gu, Y.; Burrows, D.; Moeller, K. Modern SEM-Based Mineral Liberation Analysis. *Int. J. Miner. Process.* **2007**, *84*, 310–320. [CrossRef]
181. Leppard, G.G. Size, Morphology and Composition of Particulates in Aquatic Ecosystems: Solving Speciation Problems by Correlative Electron Microscopy. *Analyst* **1992**, *117*, 595. [CrossRef] [PubMed]
182. Leppard, G.G.; Heissenberger, A.; Herndl, G.J. Ultrastructure of Marine Snow. I. Transmission Electron Microscopy Methodology. *Oceanogr. Lit. Rev.* **1997**, *1*, 25. [CrossRef]
183. Liss, S.N.; Droppo, I.G.; Flannigan, D.T.; Leppard, G.G. Floc Architecture in Wastewater and Natural Riverine Systems. *Environ. Sci. Technol.* **1996**, *30*, 680–686. [CrossRef]
184. Glauert, A.M.; Chandler, J.A. *X-Ray Microanalysis in the Electron Microscope*; North-Holland Publishing Company (Amsterdam): Amsterdam, The Netherlands, 1977.
185. Egerton, R.F. New Techniques in Electron Energy-Loss Spectroscopy and Energy-Filtered Imaging. *Micron* **2003**, *34*, 127–139. [CrossRef] [PubMed]
186. Mavrocordatos; Perret. Quantitative and Qualitative Characterization of Aquatic Iron Oxyhydroxide Particles by EF-TEM. *J. Microsc.* **1998**, *191*, 83–90. [CrossRef]
187. Liss, S.N.; Droppo, I.G.; Leppard, G.G.; Milligan, T.G. *Flocculation in Natural and Engineered Environmental Systems*; CRC Press: Boca Raton, FL, USA, 2004.
188. Filella, M. Colloidal Properties of Submicron Particles in Natural Waters. *IUPAC Ser. Anal. Phys. Chem. Environ. Syst.* **2007**, *10*, 17. [CrossRef]
189. Le Pape, P.; Quantin, C.; Morin, G.; Jouvin, D.; Kieffer, I.; Proux, O.; Ghanbaja, J.; Ayrault, S. Zinc Speciation in the Suspended Particulate Matter of an Urban River (Orge, France): Influence of Seasonality and Urbanization Gradient. *Environ. Sci. Technol.* **2014**, *48*, 11901–11909. [CrossRef] [PubMed]
190. Wilkinson, K.; Negre, J.-C.; Buffle, J. Coagulation of Colloidal Material in Surface Waters: The Role of Natural Organic Matter. *J. Contam. Hydrol.* **1997**, *26*, 229–243. [CrossRef]
191. Batista, A.H.; Melo, V.F.; Rate, A.W.; Gilkes, R.J.; Saunders, M.; Dodd, A. Scanning and Transmission Analytical Electron Microscopy (STEM-EDX) Can Identify Structural Forms of Lead by Mapping of Clay Crystals. *Geoderma* **2018**, *310*, 191–200. [CrossRef]
192. Utsunomiya, S.; Ewing, R.C. Application of High-Angle Annular Dark Field Scanning Transmission Electron Microscopy, Scanning Transmission Electron Microscopy-Energy Dispersive X-ray Spectrometry, and Energy-Filtered Transmission Electron Microscopy to the Characterization of Nanoparticles in the Environment. *Environ. Sci. Technol.* **2003**, *37*, 786–791. [CrossRef] [PubMed]
193. Sinha, A.; Ischia, G.; Straffelini, G.; Gialanella, S. A New Sample Preparation Protocol for SEM and TEM Particulate Matter Analysis. *Ultramicroscopy* **2021**, *230*, 113365. [CrossRef] [PubMed]
194. Mayer, J.; Giannuzzi, L.A.; Kamino, T.; Michael, J. TEM Sample Preparation and FIB-Induced Damage. *MRS Bull.* **2007**, *32*, 400–407. [CrossRef]

195. Fernandez, A.D.L.; Roncal-Herrero, T.; Ilett, M.; Micklethwaite, S.; Aslam, Z.; Naveed, E.; Hitchcock, J.; Cheng, C.; Lobel, B.; Cayre, O.; et al. Cryogenic Electron Microscopy for Native State Analysis of Soft- and Nano-Materials. *BIO Web Conf.* **2024**, *129*, 28006. [CrossRef]
196. Li, X.; Qin, F.; Chen, X.; Sheng, A.; Wang, Z.; Liu, J. Dissolution Behavior of Isolated and Aggregated Hematite Particles Revealed by in Situ Liquid Cell Transmission Electron Microscopy. *Environ. Sci. Technol.* **2019**, *53*, 2416–2425. [CrossRef] [PubMed]
197. Köllensperger, G.; Friedbacher, G.; Krammer, A.; Grasserbauer, M. Application of Atomic Force Microscopy to Particle Sizing. *Fresenius J. Anal. Chem.* **1999**, *363*, 323–332. [CrossRef]
198. Binnig, G.; Quate, C.F.; Gerber, C. Atomic Force Microscope. In *Scanning Tunneling Microscopy*; Springer: London, UK, 1993; pp. 55–58.
199. Scheidegger, A.M.; Sparks, D.L. A Critical Assessment of Sorption-Desorption Mechanisms at the Soil Mineral/Water Interface. *Soil Sci.* **1996**, *161*, 813–831. [CrossRef]
200. Lindgreen, H.; Garnaes, J.; Hansen, P.L.; Besenbacher, F.; Laegsgaard, E.; Stensgaard, I.; Gould, S.A.C.; Hansma, P.K. Ultrafine Particles of North Sea Illite/Smectite Clay Minerals Investigated by STM and AFM. *Am. Mineral.* **1991**, *76*, 1218–1222.
201. Liu, C.; Huang, P.M. Atomic Force Microscopy and Surface Characteristics of Iron Oxides Formed in Citrate Solutions. *Soil Sci. Soc. Am. J.* **1999**, *63*, 65–72. [CrossRef]
202. Rachlin, A.L.; Henderson, G.S.; Goh, M.C. An Atomic Force Microscope (AFM) Study of the Calcite Cleavage Plane: Image Averaging in Fourier Space. *Am. Mineral.* **1992**, *77*, 904–910.
203. Baalousha, M.; Lead, J.R. Characterization of Natural and Manufactured Nanoparticles by Atomic Force Microscopy: Effect of Analysis Mode, Environment and Sample Preparation. *Colloids Surf. A Physicochem. Eng. Asp.* **2013**, *419*, 238–247. [CrossRef]
204. Baalousha, M.; Lead, J.R. Characterization of Natural Aquatic Colloids (<5 Nm) by Flow-Field Flow Fractionation and Atomic Force Microscopy. *Environ. Sci. Technol.* **2007**, *41*, 1111–1117. [CrossRef] [PubMed]
205. Amrein, M.; Marti, O. *STM and SFM in Biology*; Academic Press: Cambridge, MA, USA, 1993.
206. Ubbink, J.; Schär-Zammaretti, P. Probing Bacterial Interactions: Integrated Approaches Combining Atomic Force Microscopy, Electron Microscopy and Biophysical Techniques. *Micron* **2005**, *36*, 293–320. [CrossRef] [PubMed]
207. Martin, M.J.; Wickramasinghe, Y.; Newson, T.P.; Crowe, J.A. Fibre-Optics and Optical Sensors in Medicine. *Med. Biol. Eng. Comput.* **1987**, *25*, 597–604. [CrossRef] [PubMed]
208. Wilkinson, K.J.; Balnois, E.; Leppard, G.G.; Buffle, J. Characteristic Features of the Major Components of Freshwater Colloidal Organic Matter Revealed by Transmission Electron and Atomic Force Microscopy. *Colloids Surf. A Physicochem. Eng. Asp.* **1999**, *155*, 287–310. [CrossRef]
209. Muirhead, D.; Lead, J.R. Measurement of the Size and Structure of Natural Aquatic Colloids in an Urbanised Watershed by Atomic Force Microscopy. *Hydrobiologia* **2003**, *494*, 65–69. [CrossRef]
210. Bickmore, B.R.; Rosso, K.M.; Nagy, K.L.; Cygan, R.T.; Tadanier, C.J. Ab Initio Determination of Edge Surface Structures for Dioctahedral 2: 1 Phyllosilicates: Implications for Acid-Base Reactivity. *Clays Clay Miner.* **2003**, *51*, 359–371. [CrossRef]
211. Macht, F.; Totsche, K.U.; Eusterhues, K.; Pronk, G.; Gilkes, R. Topography and Surface Properties of Clay Minerals Analyzed by Atomic Force Microscopy. In Proceedings of the 19th World Congress of Soil Science, Soil Solutions for a Changing World, Brisbane, Australia, 1–6 August 2010; pp. 1–6.
212. Sharp, T.G.; Oden, P.I.; Buseck, P.R. Lattice-Scale Imaging of Mica and Clay (001) Surfaces by Atomic Force Microscopy Using Net Attractive Forces. *Surf. Sci.* **1993**, *284*, L405–L410. [CrossRef]
213. Hartman, H.; Sposito, G.; Yang, A.; Manne, S.; Gould, S.A.C.; Hansma, P.K. Molecular-Scale Imaging of Clay Mineral Surfaces with the Atomic Force Microscope. *Clays Clay Miner.* **1990**, *38*, 337–342. [CrossRef]
214. Johnsson, P.A.; Eggleston, C.M.; Hochella, M.F. Imaging Molecular-Scale Structure and Microtopography of Hematite with the Atomic Force Microscope. *Am. Mineral.* **1991**, *76*, 1442–1445.
215. Wicks, F.J.; Kjoller, K.; Henderson, G.S. Imaging the Hydroxyl Surface of Lizardite at Atomic Resolution with the Atomic Force Microscope. *Can. Miner.* **1992**, *30*, 83–91.
216. Andò, S.; Garzanti, E. Raman Spectroscopy in Heavy-Mineral Studies. In *Sediment Provenance Studies in Hydrocarbon Exploration and Production*; Scott, R.A., Smyth, H.R., Morton, A.C., Richardson, N., Eds.; Geological Society, London, Special Publications 386; Geological Society: London, UK, 2013; pp. 395–412.
217. Zhang, Y.; Zhou, H.; Geng, J.; Xiao, Z.; Tu, J.; Zhang, R.; Ye, L. Identification of TiO2 Polymorphs of the Bauxite Deposit in Central Guangxi by Laser Raman Spectroscopy. *Rock Miner. Anal.* **2022**, *41*, 978–986.
218. Oliveira, M.L.S.; Saikia, B.K.; da Boit, K.; Pinto, D.; Tutikian, B.F.; Silva, L.F.O. River Dynamics and Nanopaticles Formation: A Comprehensive Study on the Nanoparticle Geochemistry of Suspended Sediments in the Magdalena River, Caribbean Industrial Area. *J. Clean. Prod.* **2019**, *213*, 819–824. [CrossRef]
219. Manceau, A.; Calas, G. Nickel-Bearing Clay Minerals: II. Intracrystalline Distribution of Nickel: An X-Ray Absorption Study. *Clay Miner.* **1986**, *21*, 341–360. [CrossRef]
220. Teo, B.K. Improvement of EXAFS Theory. In *EXAFS: Basic Principles and Data Analysis*; Springer: London, UK, 1986; pp. 79–113.

221. Priadi, C.; Le Pape, P.; Morin, G.; Ayrault, S.; Maillot, F.; Juillot, F.; Hochreutener, R.; Llorens, I.; Testemale, D.; Proux, O.; et al. X-Ray Absorption Fine Structure Evidence for Amorphous Zinc Sulfide as a Major Zinc Species in Suspended Matter from the Seine River Downstream of Paris, Ile-de-France, France. *Environ. Sci. Technol.* **2012**, *46*, 3712–3720. [CrossRef] [PubMed]
222. Churakov, S.V.; Dähn, R. Zinc Adsorption on Clays Inferred from Atomistic Simulations and EXAFS Spectroscopy. *Environ. Sci. Technol.* **2012**, *46*, 5713–5719. [CrossRef] [PubMed]
223. Dähn, R.; Scheidegger, A.M.; Manceau, A.; Curti, E.; Baeyens, B.; Bradbury, M.H.; Chateigner, D. Th Uptake on Montmorillonite: A Powder and Polarized Extended X-Ray Absorption Fine Structure (EXAFS) Study. *J. Colloid Interface Sci.* **2002**, *249*, 8–21. [CrossRef] [PubMed]
224. Lee, S.; Anderson, P.R.; Bunker, G.B.; Karanfil, C. EXAFS Study of Zn Sorption Mechanisms on Montmorillonite. *Environ. Sci. Technol.* **2004**, *38*, 5426–5432. [CrossRef] [PubMed]
225. Papelis, C.; Hayes, K.F. Distinguishing between Interlayer and External Sorption Sites of Clay Minerals Using X-Ray Absorption Spectroscopy. *Colloids Surf. A Physicochem. Eng. Asp.* **1996**, *107*, 89–96. [CrossRef]
226. Elzinga, E.J.; Rouff, A.A.; Reeder, R.J. The Long-Term Fate of Cu^{2+}, Zn^{2+}, and Pb^{2+} Adsorption Complexes at the Calcite Surface: An X-Ray Absorption Spectroscopy Study. *Geochim. Cosmochim. Acta* **2006**, *70*, 2715–2725. [CrossRef]
227. Cismasu, A.C.; Michel, F.M.; Tcaciuc, A.P.; Brown, G.E., Jr. Properties of Impurity-Bearing Ferrihydrite III. Effects of Si on the Structure of 2-Line Ferrihydrite. *Geochim. Cosmochim. Acta* **2014**, *133*, 168–185. [CrossRef]
228. Wiederhold, J.G. Metal Stable Isotope Signatures as Tracers in Environmental Geochemistry. *Environ. Sci. Technol.* **2015**, *49*, 2606–2624. [CrossRef] [PubMed]
229. Fu, Z.; Zheng, X.; Yan, Y.; Xu, X.; Zhou, F.; Li, X.; Zhou, Q.; Mai, W. The Evolution of Machine Learning in Large-Scale Mineral Prospectivity Prediction: A Decade of Innovation (2016–2025). *Minerals* **2025**, *15*, 1042. [CrossRef]
230. Juránek, R.; Výravský, J.; Kolář, M.; Motl, D.; Zemčík, P. Graph-Based Deep Learning Segmentation of EDS Spectral Images for Automated Mineral Phase Analysis. *Comput. Geosci.* **2022**, *165*, 105109. [CrossRef]
231. Li, C.; Wang, D.; Kong, L. Application of Machine Learning Techniques in Mineral Classification for Scanning Electron Microscopy-Energy Dispersive X-Ray Spectroscopy (SEM-EDS) Images. *J. Pet. Sci. Eng.* **2021**, *200*, 108178. [CrossRef]
232. Smith, R.; Spano, T.L.; McDonnell, M.; Drane, L.; Gibbs, I.; Miskowiec, A.; Niedziela, J.L.; Shields, A.E. Interpretable Machine Learning Models Classify Minerals via Spectroscopy. *Sci. Rep.* **2025**, *15*, 15807. [CrossRef] [PubMed]
233. Pan, L.; Zhang, P.; Daengngam, C.; Peng, S.; Chongcheawchamnan, M. A Review of Artificial Intelligence Methods Combined with Raman Spectroscopy to Identify the Composition of Substances. *J. Raman Spectrosc.* **2022**, *53*, 6–19. [CrossRef]
234. Wang, Q.; Xiao, J.; Li, Y.; Lu, Y.; Guo, J.; Tian, Y.; Ren, L. Mid-Level Data Fusion of Raman Spectroscopy and Laser-Induced Breakdown Spectroscopy: Improving Ores Identification Accuracy. *Anal. Chim. Acta* **2023**, *1240*, 340772. [CrossRef] [PubMed]
235. Dai, Y.; Liu, Z.; Zhao, S. Fusion of Laser-Induced Breakdown Spectroscopy and Raman Spectroscopy for Mineral Identification Based on Machine Learning. *Molecules* **2024**, *29*, 3317. [CrossRef] [PubMed]